PLOS PATHOGENS

RESEARCH ARTICLE

MAdCAM-1 costimulation in the presence of retinoic acid and TGF-β promotes HIV infection and differentiation of CD4$^+$ T cells into CCR5$^+$ T_{RM}-like cells

Sinmanus Vimonpatranon[1,2,3☯], Livia R. Goes[1,4☯], Amanda Chan[1], Isabella Licavoli[1], Jordan McMurry[1], Samuel R. Wertz[1], Anush Arakelyan[5,6], Dawei Huang[7], Andrew Jiang[1], Cindy Huang[8], Joyce Zhou[7], Jason Yolitz[1], Alexandre Girard[1], Donald Van Ryk[1], Danlan Wei[1], Il Young Hwang[1], Craig Martens[9], Kishore Kanakabandi[9], Kimmo Virtaneva[9], Stacy Ricklefs[9], Benjamin P. Darwitz[9], Marcelo A. Soares[4,10], Kovit Pattanapanyasat[2,3], Anthony S. Fauci[1], James Arthos[1‡*], Claudia Cicala[1‡*]

1 Laboratory of Immunoregulation, National Institute of Allergy and Infectious Diseases, Bethesda, Maryland, United States of America, **2** Graduate Program in Immunology, Department of Immunology, Faculty of Medicine Siriraj Hospital, Mahidol University, Bangkok, Thailand, **3** Center of Excellence for Microparticle and Exosome in Diseases, Department of Research and Development, Faculty of Medicine Siriraj Hospital, Mahidol University, Bangkok, Thailand, **4** Oncovirology Program, Instituto Nacional de Câncer, Rio de Janeiro, Brazil, **5** Eunice Kennedy-Shriver National Institute of Child Health and Human Development, Bethesda, Maryland, United States of America, **6** Georgiamune, Gaithersburg, Maryland, United States of America, **7** Lymphoid Malignancies Branch, National Cancer Institute, Bethesda, Maryland, United States of America, **8** Bioinformatics Program, St. Bonaventure University, St. Bonaventure, New York, United States of America, **9** Research Technologies Section, Genomics Unit, Rocky Mountain Laboratory, National Institutes of Allergy and Infectious Diseases, Hamilton, Montana, United States of America, **10** Department of Genetics, Universidade Federal do Rio de Janeiro, Rio de Janeiro, Brazil

☯ These authors contributed equally to this work.
‡ JA and CC also contributed equally to this work.
* jarthos@niaid.nih.gov (JA); ccicala@niaid.nih.gov (CC)

Citation: Vimonpatranon S, Goes LR, Chan A, Licavoli I, McMurry J, Wertz SR, et al. (2023) MAdCAM-1 costimulation in the presence of retinoic acid and TGF-β promotes HIV infection and differentiation of CD4$^+$ T cells into CCR5$^+$ T_{RM}-like cells. PLoS Pathog 19(3): e1011209. https://doi.org/10.1371/journal.ppat.1011209

Editor: Guido Silvestri, Emory University, UNITED STATES

Received: August 23, 2022

Accepted: February 15, 2023

Published: March 10, 2023

Data Availability Statement: This study included the generation of gene expression data (RNASeq). This data has been deposited in the GSEA data base, under accession # GSE221434. You can acclaim this accession https://www.ncbi.nlm.nih.gov/geo/query/acc.cgi?acc=GSE221434.

Funding: This work was supported by the Division of Intramural Research, National Institute of Allergy and Infectious Diseases; Thailand Research Fund, The Royal Golden Jubilee (RGJ) PhD Program

Abstract

CD4$^+$ tissue resident memory T cells (T_{RM}s) are implicated in the formation of persistent HIV reservoirs that are established during the very early stages of infection. The tissue-specific factors that direct T cells to establish tissue residency are not well defined, nor are the factors that establish viral latency. We report that costimulation via MAdCAM-1 and retinoic acid (RA), two constituents of gut tissues, together with TGF-β, promote the differentiation of CD4$^+$ T cells into a distinct subset $\alpha_4\beta_7{}^+$CD69$^+$CD103$^+$ T_{RM}-like cells. Among the costimulatory ligands we evaluated, MAdCAM-1 was unique in its capacity to upregulate both CCR5 and CCR9. MAdCAM-1 costimulation rendered cells susceptible to HIV infection. Differentiation of T_{RM}-like cells was reduced by MAdCAM-1 antagonists developed to treat inflammatory bowel diseases. These finding provide a framework to better understand the contribution of CD4$^+$ T_{RM}s to persistent viral reservoirs and HIV pathogenesis.

(PHD/0027/2557 to SV) and Carlos Chagas Filho Rio de Janeiro State Science Foundation (FAPERJ – E-40/ 200.584/2022 to LG). The funders had no role in study design, data collection and analysis, decision to publish, or preparation of the manuscript.

Competing interests: The authors have declared that no competing interests exist.

Author summary

Although antiretroviral drugs strongly suppress viral replication in HIV infected subjects, viral reservoirs persist. To achieve a cure, these reservoirs need to be eliminated. However, the location and identity of persistently infected cells are not well understood. Tissue resident memory $CD4^+$ T cells (T_{RM}s) are a cell type that may play an important role. These cells reside in tissues for extended periods of time and circulate infrequently. To increase our understanding of the role of T_{RM}s in HIV reservoirs this study identifies MAdCAM-1 and retinoic acid (RA) as two key components of the gut immune system involved in the generation of T_{RM}s. Treatment of primary $CD4^+$ T cells with MAdCAM-1 and RA renders cells susceptible to HIV infection and primes them to adopt a T_{RM}-like phenotype. Addition of a TGF-β, an anti-proliferative cytokine, induces them to adopt a more complete T_{RM}-like phenotype. This study provides a new approach toward studying the persistent reservoirs that are a barrier to an HIV cure.

Introduction

In the early stages of HIV infection, gut inductive lymphoid sites, including Peyer's patches, are preferentially targeted. The consequent damage to gut-associated lymphoid tissues (GALT) plays a significant role in HIV pathogenesis [1–5]. Trafficking of naïve $CD4^+$ T cells to these inductive sites is mediated by a series of interactions involving T cell homing receptors and their cognate ligands [6,7]. Integrin $\alpha_4\beta_7$ ($\alpha_4\beta_7$) and MAdCAM-1 play a central role in this process. MAdCAM-1 binding to $\alpha_4\beta_7$ delivers a costimulatory signal to $\alpha_4\beta_7$-expressing $CD4^+$ T cells, including naïve $CD4^+$ T cells [8,9]. We previously reported that, unlike memory $CD4^+$ T cells, MAdCAM-1-dependent proliferation of naïve $CD4^+$ T cells requires the addition of retinoic acid (RA), a vitamin A metabolite that is generated by dendritic cells in Peyer's patches [9].

The combination of MAdCAM-1 and RA induces a distinct differentiation program in naïve $CD4^+$ T cells that leads to the generation of $CD4^+$ T cells with an $\alpha_4\beta_7^{high}$ phenotype that supports viral replication [9]. We suggested that the combination of MAdCAM-1 and RA, which is primarily localized to GALT and genital mucosa, might contribute to the gut-tropic nature of HIV in the acute phase of infection. Like MAdCAM-1, the V2 domain of the gp120 HIV envelope protein binds to and signals through $\alpha_4\beta_7$ [10–12]. This activity may also contribute to HIV gut tropism.

What remained unclear from the above-mentioned studies was the manner in which naïve $CD4^+$ T cells differentiated following MAdCAM-1 + RA costimulation. Depending upon various factors, such costimulation can drive $CD4^+$ T cells toward a central memory (T_{CM}) or effector memory (T_{EM}) phenotype. In the past decade, a third memory T cell subset, identified as tissue resident memory T cells (T_{RM}), has been described [13–16]. Because these cells reside primarily in tissues and circulate infrequently, they are difficult to harvest, and their role in HIV pathogenesis is less well defined. Several studies have suggested that T_{RM}s may contribute to the formation of persistent viral reservoirs [17–20]. In this study we determined that MAdCAM-1 + RA can, in combination with TGF-β, promote the formation of $CCR5^+$ cells bearing a T_{RM}-like phenotype, similar to the $CCR5^+$ T_{RM}s that Prilc and colleagues recently identified in human rectal mucosa [21]. By demonstrating that factors associated with the gut tissue milieu can drive $CD4^+$ T cells to adopt a T_{RM}-like cell phenotype, this study provides a basis to better define the role of T_{RM}s in HIV pathogenesis.

Results

RNA transcription profile in MAdCAM-1 and gp120 V2 costimulated CD4+ T cells

In previous studies we reported that purified $CD4^+$ T cell cultures derived from healthy donor PBMCs proliferated when costimulated with a CD3 antibody (Ab) and MAdCAM-1-Ig (MAdCAM-1) [9]. Costimulation with a cyclic peptide derived from the V2 loop of gp120 (cV2) also drove $CD4^+$ T cell proliferation [11]. Starting cultures were typically comprised of ~40–60% naïve T cells, with the remainder comprised of memory cell subsets. Of note, purified naïve $CD4^+$ T cell cultures could also proliferate, but only if RA was added to culture supernatants [9]. To better understand the $CD4^+$ T cell differentiation program driven by MAdCAM-1 + RA or cV2 + RA, we carried out gene expression profiling by RNA-Seq. Primary $CD4^+$ T cells were isolated from the PBMCs of 6 healthy donors. Cultures were stimulated with a CD3 Ab in the presence of either MAdCAM-1 or cV2 as previously described [9,11]. For comparison, we also stimulated cells with CD3 Ab alone and CD3 Ab in combination with a CD28 Ab. All treatments were performed in the presence or absence of RA. Cells were harvested and RNA was isolated at 24 and 48 hrs. Bulk RNA-Seq results and an RNA-Seq analysis pipeline were used to generate genome-wide gene expression profiles. The RNA-Seq gene expression values we obtained represent the combined signals from all cell subsets. We then analyzed this gene-expression data set with CIBERSORT, a recently improved bioinformatics tool, in conjunction with a customized reference matrix of leukocyte cell type signature genes derived from previously published gene expression profiles [22,23]. In our customized matrix, ITGAE was employed as the defining maker of T_{RM} cells. Additional details are included in the methods section. CIBERSORT provided an estimate of the T cell subset composition ratios in each of our bulk RNA-Seq samples. We noted a marked enrichment of T_{RM} cell ratios in the MAdCAM-1 + RA treatment group (Fig 1A and S1 Table). In an unsupervised genome-wide gene set enrichment analysis (GSEA) [24], the term T_{RM} ranked at the top of biological terms in the MAdCAM-1 + RA treatment group, but not in the CD28 Ab treatment group (S2 Table). To validate these findings, we examined the transcription of the two markers most frequently used to define T_{RM} cells: CD103 and CD69 [25,26]. CD103 (integrin α_E) forms a heterodimer exclusively with integrin β_7 [27], and its expression is indicative of $\alpha_E\beta_7$ positivity. $\alpha_E\beta_7$ facilitates retention of T cells in gut tissues [26,28]. Transcription of ITGAE (CD103 gene) was upregulated ~3-fold by MAdCAM-1, in either the presence or absence of RA, while CD28 Ab and cV2 showed a ~2-fold increase (Fig 1B). The 2nd marker, CD69, is a C-type lectin that is considered an early but transient marker of T cell activation. However, prolonged expression of CD69 is a hallmark of T_{RM} cells [25]. At 24 hrs after MAdCAM-1 stimulation, CD69 transcription showed a ~5-fold increase, in either the presence or absence of RA (Fig 1C). Stimulation with either CD28 Ab or cV2 showed a more modest (~2-4-fold) increase in CD69 transcription. These findings prompted us to interrogate our RNA-Seq results with an extended panel of genes associated with T_{RM} cells. From 53 recent publications we composed a database of 99 genes associated with T_{RM}s (S3 Table). Of these, 45 were strongly associated with T_{RM}s (see methods section). We next generated a gene expression heatmap for 40 of these genes that were modulated by CD3 Ab + MAdCAM-1 + RA stimulation relative to CD3 Ab stimulation alone (Fig 1D). In most instances, all six donors either increased or decreased transcription of these genes in a manner consistent with T_{RM} cell gene expression. Three genes whose expression level appeared to be modulated were selected and independently confirmed by RT-qPCR (S1A Fig).

T cell differentiation is regulated, in part, by transcription factors (TFs). Several TF genes linked to T_{RM} differentiation were modulated in our RNA-seq data set in a way that is consistent with differentiation toward a T_{RM} phenotype. A schematic of TF gene modulation is

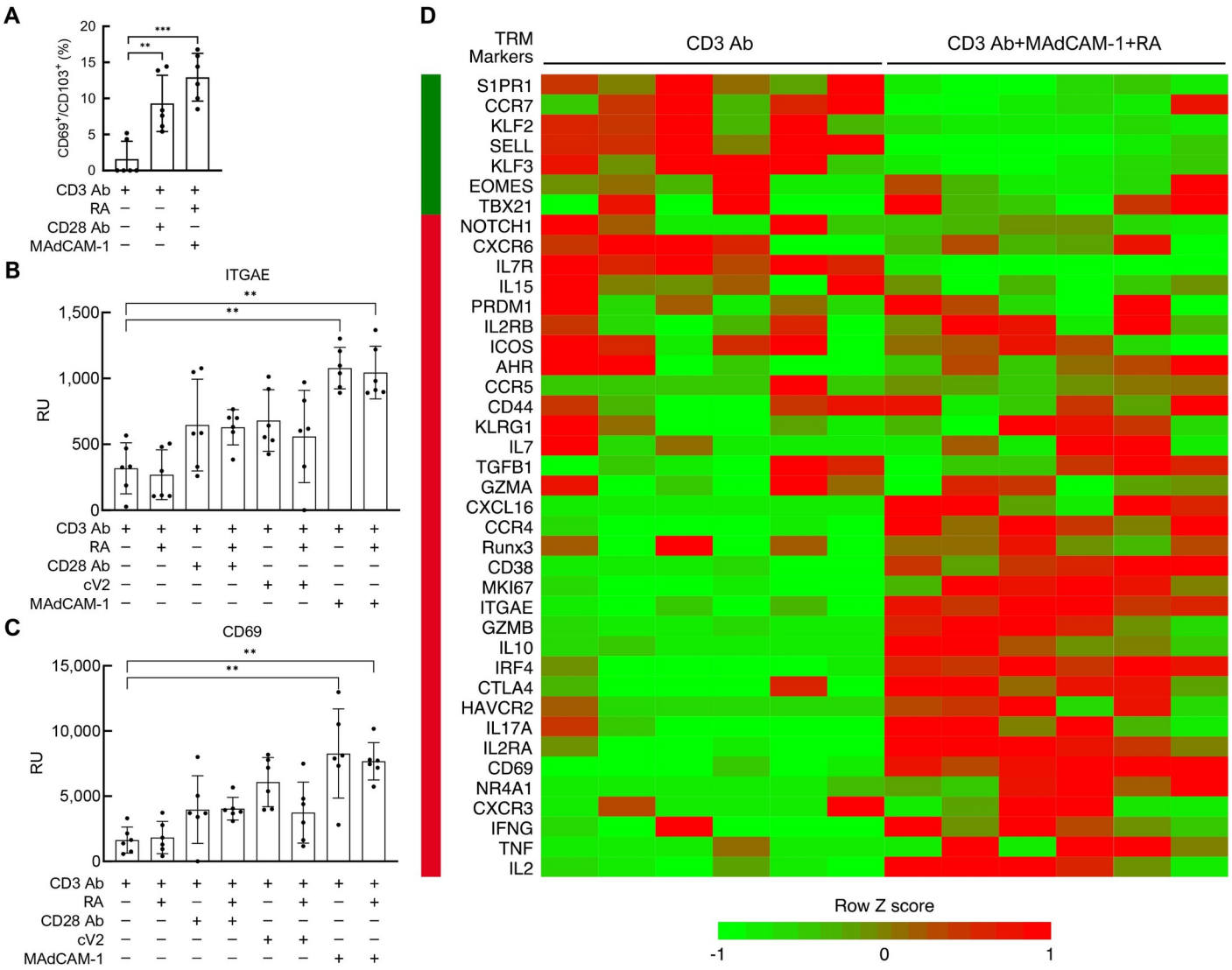

Fig 1. Transcription profile of MAdCAM-1 costimulated CD4+ T cells. (**A**) % $CD69^+/CD103^+$composition in bulk RNA-Seq samples stimulated with CD3 Ab, CD3 Ab + CD28 Ab, and CD3 Ab + MAdCAM-1 + RA as estimated by CIBERSORT. Average (**B**) ITGAE and (**C**) CD69 RNA levels from $CD4^+$ T cells of 6 donors costimulated with CD3 Ab alone, CD3 Ab + cV2, CD3 Ab + MAdCAM-1, and CD3 Ab + CD28 Ab in the presence or absence of RA, detected by RNA-Seq. Y-axis represents relative units. Error bars indicate SD. (**D**) Heatmap comparing average RNA expression levels from 6 donors for 40 selected genes associated with T_{RM} cells following stimulation with CD3 Ab vs CD3 Ab + MAdCAM-1 + RA. Each column represents one donor, each row represents a selected gene. Side bar indicates direction of gene modulation (green: decrease, red: increase) in T_{RM}s, as previously reported. (*: $P < 0.05$, **: $P < 0.01$, ***: $P < 0.001$ two-tailed t test).

https://doi.org/10.1371/journal.ppat.1011209.g001

presented in S1B Fig. T-Bet, Nurr77, and Ahr were upregulated, while Eomes, TCF1, and KLF2 were downregulated [29–38].

A subset of T_{RM} cells in mucosal tissues exhibits a Th17 phenotype that includes the production of IL-17, IFN-γ, IL-21 and IL-22 [21,39,40]. We observed increased transcription of IL17A in 5 of 6 donors (Fig 1D). This result prompted us to carry out a multiplex cytokine analysis of culture supernatants. We compared cytokine secretion following MAdCAM-1 or cV2 costimulation in the absence vs. presence of RA. Both induced low-level secretion of IL-17F and IFN-γ in the absence of RA. These levels were increased markedly in the presence of RA (S2 and S3 Figs). MAdCAM-1 induced TNF-α secretion ~10-fold in the presence of RA. IL-2, which fell below the limit of detection (4 pg/ml) in cells stimulated with MAdCAM-1 in

the absence of RA, increased secretion to ~900 pg/ml in the presence of RA. Similarly, MAdCAM-1 induced IL-21 in the presence of RA.

From these analyses we conclude that both MAdCAM-1 and cV2 costimulation mediate a generally similar response, in agreement with our previous studies [9,11]. MAdCAM-1 appeared to provide a stronger stimulus. Treatment with MAdCAM-1, and particularly the combination of MAdCAM-1 + RA, induced cells to adopt a T_{RM}-like transcription profile. Gene expression analyses can be error-prone. We therefore tentatively concluded that MAdCAM-1 + RA might be priming cells to adopt a gene expression program consistent with T_{RM} differentiation. To strengthen this conclusion we next asked whether the canonical signatures of T_{RM} cells were present on MAdCAM-1 + RA costimulated cultures of primary $CD4^+$ T cells.

Induction of CD69, CD103, CCR9 and CCR5

We began our phenotypic analysis of MAdCAM-1 + RA costimulated $CD4^+$ T cells by evaluating the cell-surface expression of CD69 and CD103. Because TGF-β is known to modulate CD103 expression [41], we also included cultures with MAdCAM-1 + RA + TGF-β. Bulk $CD4^+$ T cells were isolated from PBMCs and placed into wells coated with CD3 Ab and MAdCAM-1. For comparison, we included control cultures costimulated with a CD28 Ab and VCAM-Ig (VCAM-1). VCAM-1 delivers costimulatory signals through $\alpha_4\beta_7$, but also through $\alpha_4\beta_1$, which is expressed ubiquitously on peripheral $CD4^+$ T cells [42,43]. RA was included in all cultures. Cells were initially stimulated for 4 days in the absence of TGF-β (Fig 2A). On day 4, culture media was renewed and TGF-β was added where indicated. Cells were harvested on day 7 and multicolor flow-cytometric analysis was performed. A representative result of CD69 and CD103 expression following stimulation with CD3 Ab, CD3 Ab + MAdCAM-1, CD3 Ab + TGF-β, and CD3 Ab + MAdCAM-1 + TGF-β, all in the presence of RA is shown in Fig 2B. In 21 independent donors, the addition of MAdCAM-1 + RA was sufficient to induce a low but significant number of $CD69^+/CD103^+$ cells (average 5.9%) (Fig 2C). With the addition of TGF-β, all three costimulatory ligands induced the co-expression of CD69 and CD103 on a subset of cells. Because CD69/CD103 co-expression is a hallmark of T_{RM} cells, herein we refer to these cells as T_{RM}-like, recognizing, as discussed below, that this is an approximation. The capacity of MAdCAM-1 to induce the surface expression of both CD69 and CD103 agrees with the increased transcription of these genes described above. In the presence of RA, all three costimulatory ligands mediated increased expression of $\alpha_4\beta_7$, both in the absence and presence of TGF-β (S4A Fig). Under certain conditions, $\alpha_4\beta_7$ expression is reportedly downregulated when CD103, in the form of $\alpha_E\beta_7$, appears on the cell surface [28,44]; however, we found that, in the presence of RA and TGF-β, $\alpha_4\beta_7$ expression was retained on the majority of $CD69^+/CD103^+$ (i.e. $CD69^+/\alpha_E\beta_7^+$) cells (S4B Fig). We next evaluated the expression of two chemokine receptors, CCR5 and CCR9, on MAdCAM-1-derived T_{RM}-like cells. CCR9 is the gut homing chemokine receptor [45] and has been described as a marker of gut T_{RM}s [46]. CCR5 is the HIV coreceptor most frequently utilized in the early stages of infection [47]. Cells were costimulated in the presence of RA + TGF-β as described above. In 16 donors, MAdCAM-1 costimulation resulted in a significantly higher level of both CCR5 and CCR9 on T_{RM}-like cells relative to either VCAM-1 or CD28 Ab costimulation (Figs 2D and 2E and S5). Upregulation of CCR5 may render cells susceptible to HIV infection (see below).

We next asked whether CCR9 and CCR5 were co-expressed or appeared on different subsets of $CD69^+/CD103^+$ cells. Expression was evaluated at days 5, 7, and 9 following MAdCAM-1 + RA + TGF-β stimulation. Maximum CCR9 and CCR5 expression occurred on day 7 and 9, respectively (Fig 2F). Of note, within the time points we measured the majority of cells expressed either chemokine receptor, with only a minority of cells expressing both.

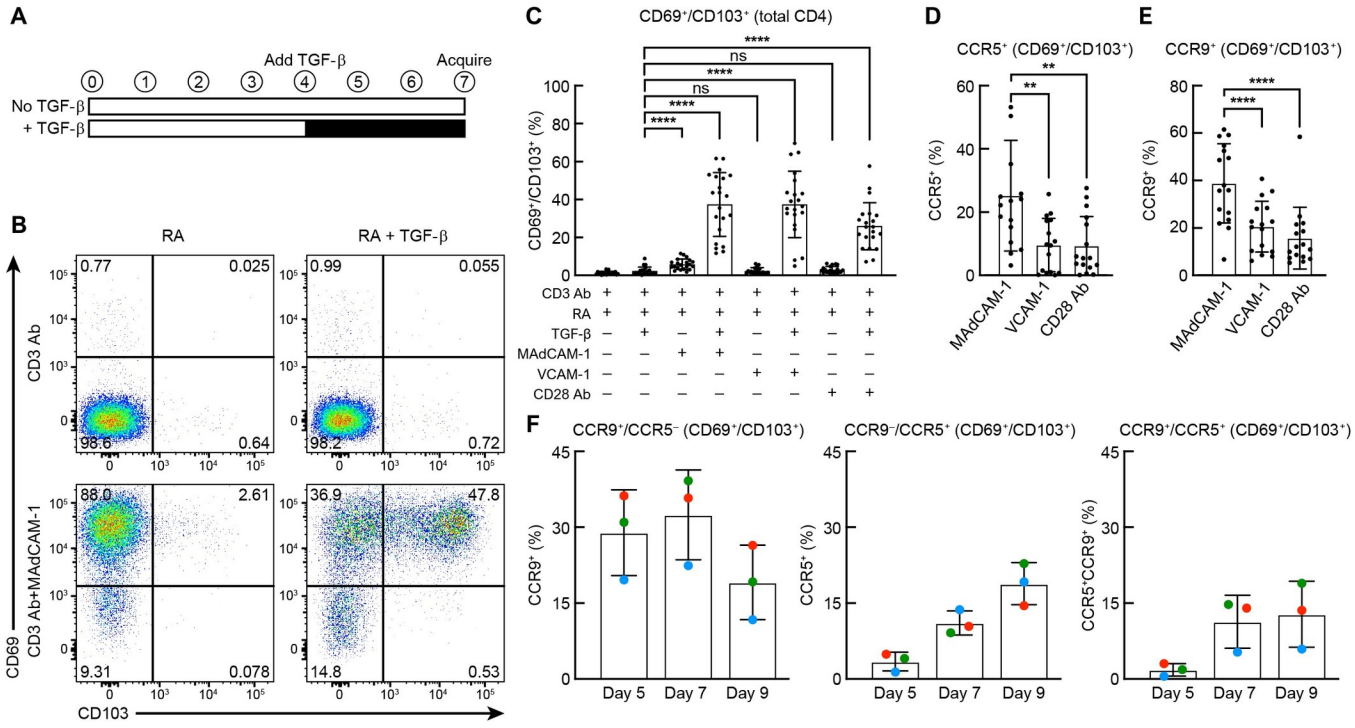

Fig 2. Induction of CD69, CD103, CCR9 and CCR5. (**A**) Schematic of treatment time course. (**B**) Representative flow cytometry dot plot of CD4+ T cells stimulated with CD3 Ab, and CD3 Ab + MAdCAM-1 in presence of RA or RA+TGF-β as indicated. Y-axis: CD69, X-axis: CD103. Percent total cells in each quadrant, as indicated. (**C**) Percent expression of $CD69^+/CD103^+$ cells within total $CD4^+$ T cell cultures of 21 donors stimulated with CD3 Ab + RA, CD3 Ab + MAdCAM-1 + RA, CD3 Ab + VCAM-1 +RA, and CD3 Ab + CD28 Ab + RA, in absence or presence of TGF-β, as indicated. (**D**) Percent expression of CCR5 and (**E**) CCR9 within the $CD69^+/CD103^+$ population of 16 donors following MAdCAM-1, VCAM-1 and CD28 Ab stimulation in the presence of RA and TGF-β. (**F**) Percent expression of $CCR9^+/CCR5^-$, $CCR9^-/CCR5^+$, and $CCR9^+/CCR5^+$ cells within the $CD69^+/CD103^+$ population from 3 donors on days 5, 7, and 9 following MAdCAM-1 + RA + TGF-β stimulation. (**: $P < 0.01$, ****: $P < 0.0001$, two-tailed t test).

https://doi.org/10.1371/journal.ppat.1011209.g002

In summary, MAdCAM-1, in the absence of TGF-β, promoted the formation of a subset of cells with a $CD69^+/CD103^+$ phenotype. The frequency of these cells increased with the addition of TGF-β. CD28 Ab and VCAM-1 also induced T_{RM}-like cells but only in the presence of TGF-β. In the presence of RA and TGF-β, MAdCAM-1-derived T_{RM}-like cells expressed higher levels of either CCR9 or CCR5 in comparison to VCAM-1 or CD28 Ab stimulated cells.

CD28 Ab but not MAdCAM-1 or VCAM-1 induces Tregs

TGF-β and RA have been reported to work together to drive cells toward a Treg phenotype [48–51]. We asked whether MAdCAM-1 + RA + TGF-β resulted in a differentiation pattern consistent with Tregs. Cells were costimulated with MAdCAM-1, VCAM-1, or CD28 Ab as described above and stained for intracellular FoxP3 and CD25, two markers associated with Tregs (Fig 3A). However, a $FoxP3^+/CD25^+$ phenotype is not always reflective of Treg function and should be considered in that regard. As described by others, costimulation with CD28 Ab + RA yielded a ~6-fold increase in $FoxP3^+/CD25^+$ cells relative to CD3 Ab + RA. This upregulation was enhanced further by the addition of TGF-β. Surprisingly, neither MAdCAM-1 + RA nor VCAM-1 + RA, with or without TGF-β, mediated a significant increase in the frequency of $FoxP3^+/CD25^+$ cells. This pattern held true within the T_{RM}-like cell subpopulation (Fig 3B). In mucosal tissues, Tregs exhibit increased FoxP3 and CTLA-4 expression when compared to circulating Tregs [21]. We found that CTLA-4 was upregulated on T_{RM}-like cells induced by CD28 Ab + RA + TGF-β, and to a lesser extent on MAdCAM-1 and VCAM-1

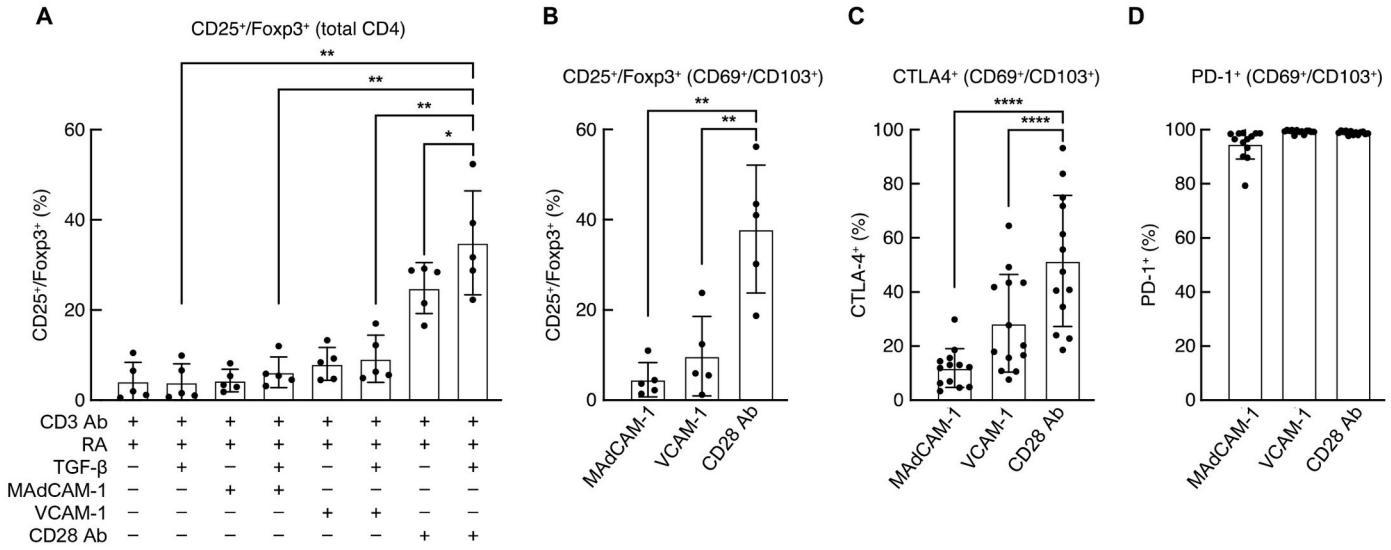

Fig 3. CD25/FoxP3, PD-1 and CTLA-4 expression following costimulation. Flow cytometric analysis of (**A**) CD25/FoxP3 co-expression on total CD4$^+$ T cells following costimulation with MAdCAM-1, VCAM-1 and CD28 Ab in the presence of RA and TGF-β as indicated (n = 5). Expression of (**B**) CD25/FoxP3 (n = 5), (**C**) CTLA-4 (n = 13), and (**D**) PD-1 (n = 13) within the CD69$^+$/CD103$^+$ population following costimulation with MAdCAM-1, VCAM-1 and CD28 Ab, in the presence of RA and TGF-β (*: $P < 0.05$, **: $P < 0.01$, ****: $P < 0.0001$, two-tailed t test).

https://doi.org/10.1371/journal.ppat.1011209.g003

costimulated cells (Fig 3C). Finally, we found that all three costimulatory ligands, when combined with RA and TGF-β, induced similarly high levels of PD-1 on T_{RM}-like cells (Fig 3D). The failure of MAdCAM-1 and VCAM-1 to induce the expression of FoxP3 and CD25 underscores the way in which different costimulatory signals can influence cell differentiation in critical ways.

We noted above that five of six donor CD4$^+$ T cells exhibited increased transcription of IL17A (Fig 1D). We followed this observation by measuring the secretion of cytokines with a multiplex cytokine array. The combination of MAdCAM-1 + RA induced the secretion of IL-17F and IFN-γ (S2 and S3 Figs). These measurements were made at time points prior to TGF-β treatment, which we carry out on day 4 following costimulation. This prompted us to address the type of cell polarization induced by MAdCAM-1 + RA following TGF-β treatment. To this end, we measured surface expression markers associated with Th17 (CCR6) and Th1 (CXCR3) on day 7 by flow cytometry. Approximately half of the CD69$^+$/CD103$^+$ cells expressed CXCR3. Only low levels of CCR6 were observed (S6 Fig). These data indicate IL-17 production prior to the addition of TGF-β and suggest a degree of Th1 polarization on day 7. Th polarization is highly plastic [52–54] and our findings are consistent with such plasticity.

Role of RA and TGF-β in MAdCAM-1 generation of CD4$^+$ T_{RM}-like cells

MAdCAM-1 can signal through $\alpha_4\beta_7$ but not through $\alpha_E\beta_7$. RA increases the surface expression of $\alpha_4\beta_7$ by upregulating integrin β_7 (ITGB7) [45]. TGF-β upregulates integrin α_E (CD103) which pairs exclusively with integrin β_7 [41]. With this dynamic in mind, we compared the impact of RA vs TGF-β on MAdCAM-1-mediated induction of CD69$^+$/CD103$^+$ T_{RM}-like cells. Cells were costimulated and analyzed for CD69 and CD103 expression, as described above. A representative comparison of MAdCAM-1 costimulation with all four combinations of RA and TGF-β is presented (Fig 4A), along with results from four donors stimulated with each of the three costimulatory ligands (Fig 4B). CD3 Ab + MAdCAM-1 alone, or in the presence of either RA or TGF-β, induced cells presenting a CD69$^+$/CD103$^+$ phenotype at a low frequency (~4–

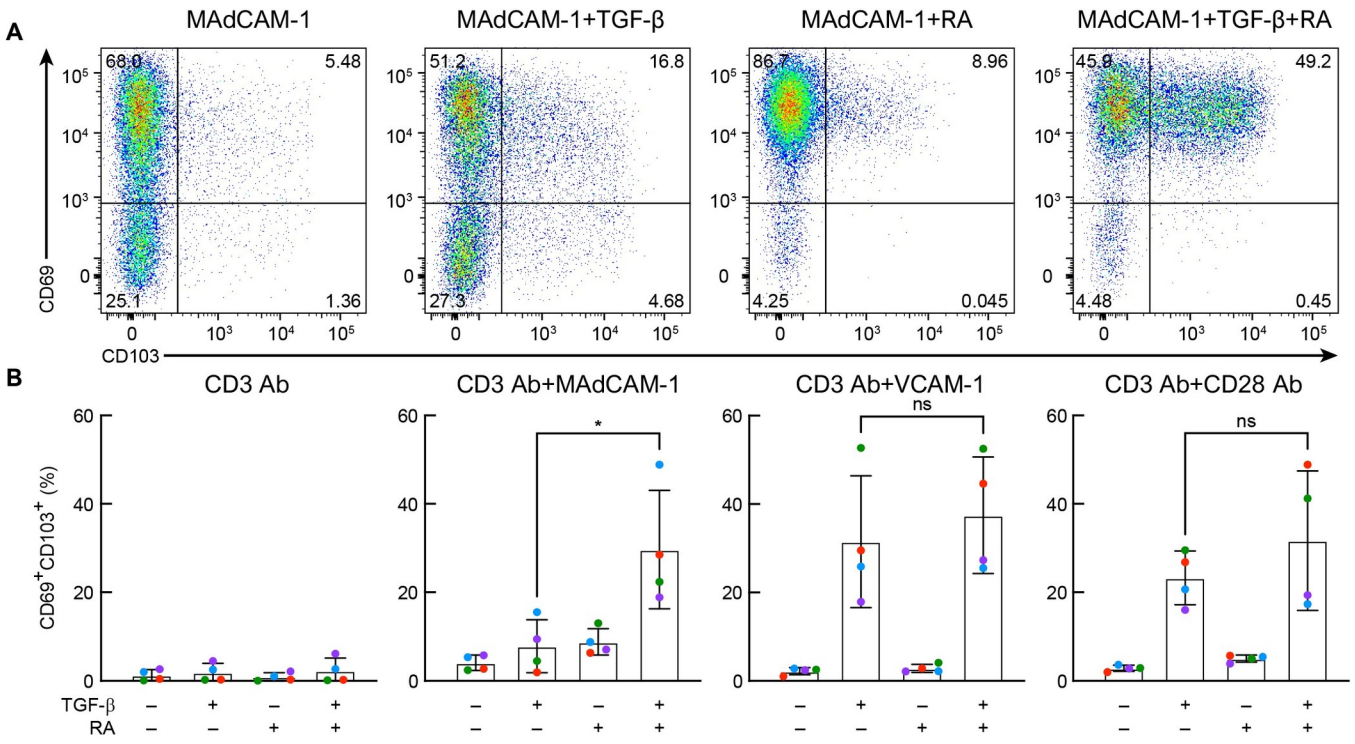

Fig 4. Effect of RA and TGF-β on CD69⁺/CD103⁺ expression. (**A**) Representative flow cytometry dot plot of CD69 (Y-axis) and CD103 (X-axis) on CD3 Ab + MAdCAM-1 stimulated CD4⁺ T cells in the absence or presence of RA and TGF-β, as indicated. Percent of total cells in each quadrant, as indicated. (**B**) Average percent CD69⁺/CD103⁺ cells following CD3 Ab alone, CD3 Ab + MAdCAM-1, CD3 Ab + VCAM-1 or CD3 Ab + CD28 Ab stimulation in the absence or presence of RA and TGF-β as indicated (n = 4). (*: $P < 0.05$, two-tailed t test).

https://doi.org/10.1371/journal.ppat.1011209.g004

9%). Combining MAdCAM-1 + RA + TGF-β increased significantly the frequency of T_{RM}-like cells. These results suggest that, in the absence of RA, low levels of integrin β_7 on the cell surface limit the formation of $\alpha_4\beta_7$, which in turn limits MAdCAM-1-mediated costimulation. The combination of RA and TGF-β allows cells to respond to MAdCAM-1, while concomitantly upregulating CD103. VCAM-1 and CD28 Ab can costimulate cells independently of $\alpha_4\beta_7$, and they require only TGF-β to induce T_{RM}s. These observations underscore the way in which MAdCAM-1 and RA, a combination that is linked to the gut milieu, when combined with TGF-β, can promote the formation of relatively high levels of CD69⁺/CD103⁺ T_{RM}-like cells. T_{RM}-like cells induced by MAdCAM-1 costimulation exhibit properties distinct from those generated by CD28 Ab and VCAM-1, as will be further described below.

Influence of RA and TGF-β on CCR5 and CCR9 expression

The capacity of RA to induce the expression of both CCR9 and $\alpha_4\beta_7$ underlies its role in CD4⁺ T cell trafficking to GALT [45]. Less understood is the effect of combining RA with TGF-β on CCR5 and CCR9 expression. To address this issue, CD4⁺ T cells were costimulated with MAdCAM-1 + RA, VCAM-1 + RA and CD28 Ab + RA as described above in the absence or presence of TGF-β. CCR5 and CCR9 expression in the total CD4⁺ T cell population, and within the CD69⁺/CD103⁺ population, were determined on day 7. Surprisingly, in 16 independent donors, the addition of TGF-β to cells stimulated with MAdCAM-1 + RA increased the frequency of CCR5 expressing cells by an average ~1.5-fold (Fig 5A). This increase also appeared within the CD69⁺/CD103⁺ subpopulation (Fig 5B). TGF-β did not increase CCR5 expression in VCAM-1 + RA or CD28 Ab + RA treated cells. To our knowledge, this effect of combining

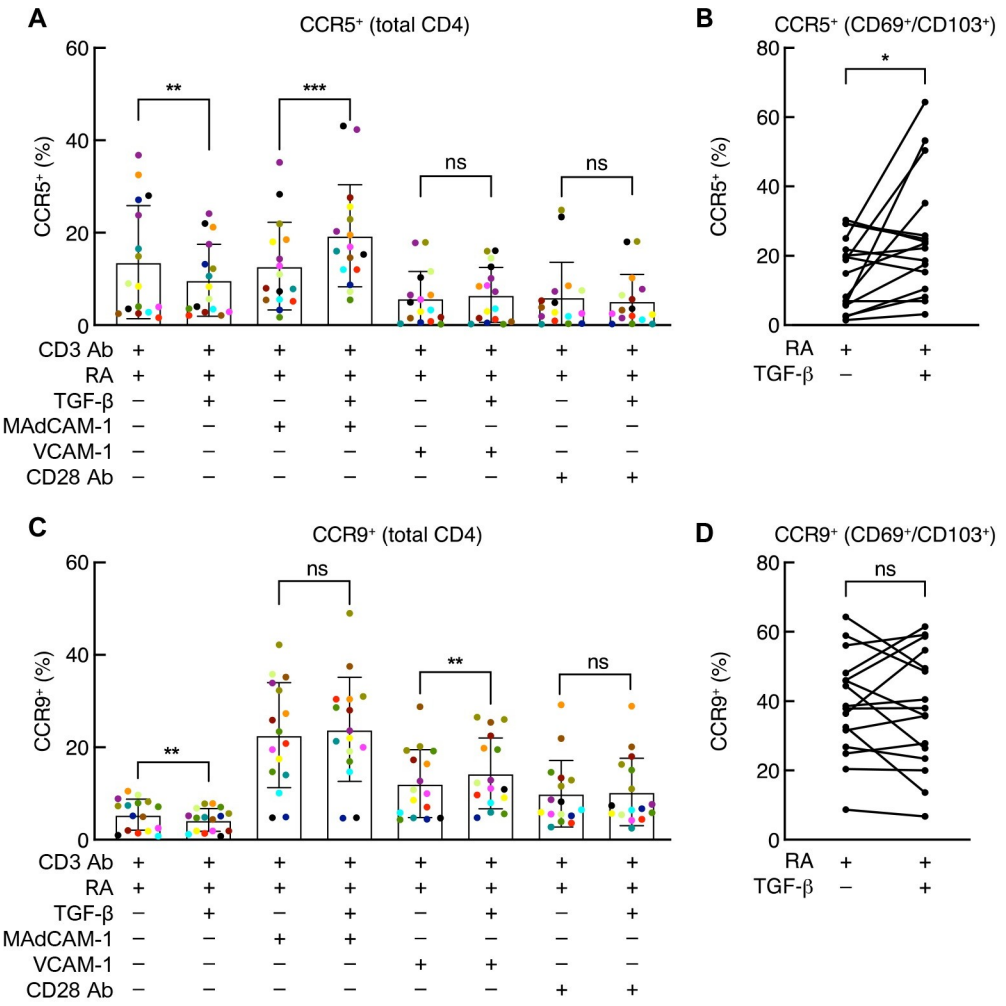

Fig 5. TGF-β effect on CCR5 and CCR9 expression. Flow-cytometric analysis of CCR5 and CCR9 expression on total $CD4^+$ T cells (**A** and **C**) or $CD69^+/CD103^+$ $CD4^+$ T cells (**B** and **D**) costimulated with MAdCAM-1 + RA, VCAM-1 + RA, or CD28 Ab + RA, in the absence or presence of TGF-β, as indicated (n = 16) (*: $P < 0.05$, **: $P < 0.01$, ***: $P < 0.001$, two-tailed t test).

https://doi.org/10.1371/journal.ppat.1011209.g005

TGF-β with MAdCAM-1 has not been previously observed. TGF-β had little impact on the expression of CCR9 on $CD4^+$ T cells for any of the three costimulatory ligands, either in the total $CD4^+$ T cell population or in the MAdCAM-1 + RA treated $CD69^+/CD103^+$ subpopulation (Fig 5C and 5D). In summary, in the presence of RA, TGF-β increased the expression of CCR5 on $CD4^+$ T cells, including on $CD69^+/CD103^+$ T_{RM}-like cells. For $CD69^+/CD103^+$ cells, this effect was observed only in the context of MAdCAM-1 costimulation, underscoring the distinct way in which combining MAdCAM-1 with RA and TGF-β impacts the differentiation of $CD4^+$ T cells.

$\alpha_4\beta_7$ antagonists inhibit the differentiation of $CD4^+$ T cells into T_{RM}-like cells

Vedolizumab is a humanized $\alpha_4\beta_7$ mAb that interferes with MAdCAM-1 binding. In recent years it has become a front-line therapeutic in the treatment of inflammatory bowel diseases (IBD) [55]. Subsequently, related antagonists have been developed as alternative therapies.

Etrolizumab, which targets integrin β_7, is a humanized derivative of FIB504, a mouse mAb specific to integrin β_7 [56]. Ontamalimab (PF-00547659) is a human MAdCAM-1 Ab [57,58]. Although the initial rationale for employing these mAbs in the treatment of IBD involved their potential to inhibit $CD4^+$ T cell migration into GALT, recent data suggest that their mode of action may involve other mechanisms [9,59–61]. We asked whether vedolizumab along with a primatized FIB504 (β_7 Ab) and the 314G8 (MAdCAM-1 Ab) [62], with a specificity similar to ontamalimab, could inhibit the formation of T_{RM}-like cells. Cells were costimulated with MAdCAM-1 + RA as described above. On day 4, TGF-β was added with or without each of the three mAb antagonists. All three mAbs inhibited $CD69^+/CD103^+$ T_{RM}-like cell differentiation in a significant way (Fig 6A and 6B). In six independent donors, vedolizumab, β_7 Ab, and MAdCAM-1 Ab each inhibited T_{RM}-like cell differentiation by ~65%, while a control mAb showed no significant inhibition. There were several ways in which these $\alpha_4\beta_7$ antagonists altered cell phenotypes in unexpected ways. $CD69^-/CD103^+$ cells typically appear at a low frequency following MAdCAM-1 + RA + TGF-β stimulation. Interestingly, all three $\alpha_4\beta_7$ antagonists increased the frequency of $CD69^-/CD103^+$ cells by ~2-fold (Fig 6C). Additionally, all three antagonists failed to reduce the expression of either CCR9 or CCR5 (Figs 6D and S7A and S7B). Finally, we found that MAdCAM-1 Ab did not reduce the expression of integrin β_7 (S7C Fig).

HIV infection in T_{RM}s

The capacity of TGF-β, when combined with RA, to induce CCR5 on MAdCAM-1-derived T_{RM}-like cells raised the possibility that MAdCAM-1+ RA costimulation might support HIV

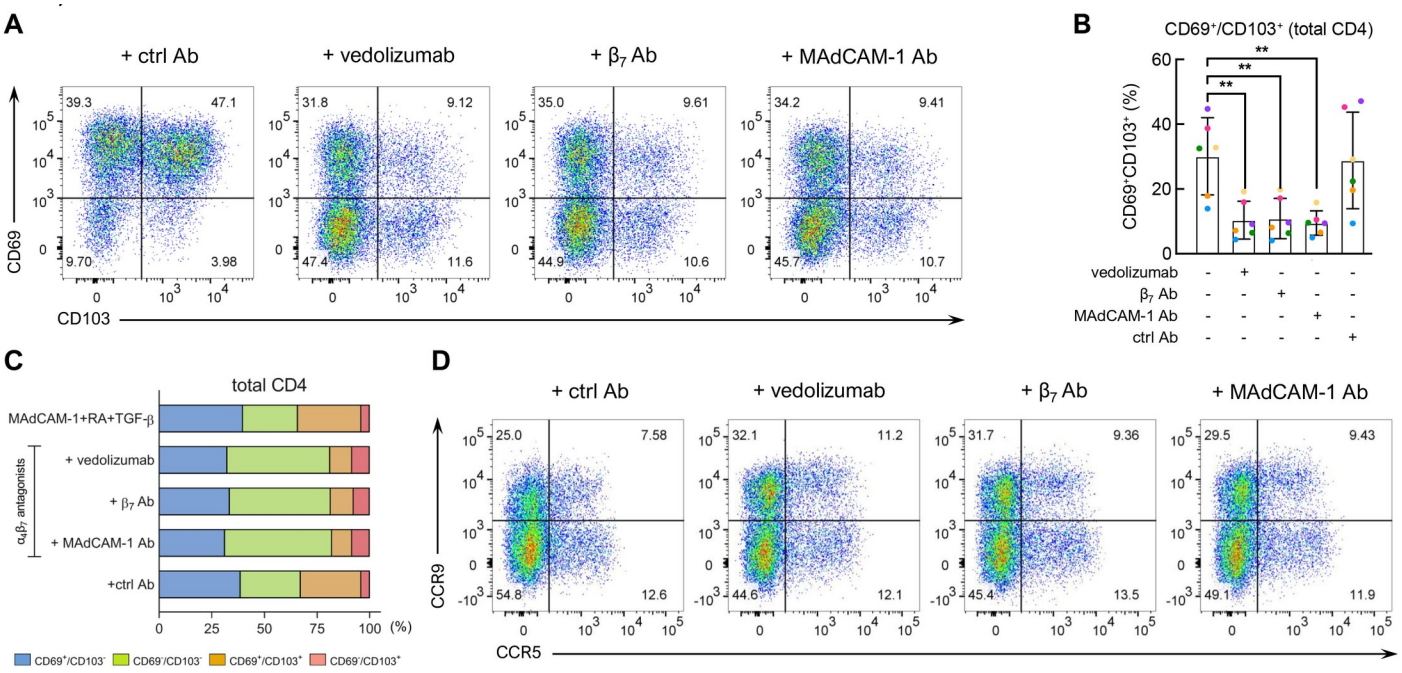

Fig 6. $\alpha_4\beta_7$ antagonists inhibit T_{RM}-like cell differentiation. (**A**) Representative flow cytometry dot plot of CD69 (Y-axis) and CD103 (X-axis) expression following costimulation with MAdCAM-1 + RA + TGF-β in the absence or presence of vedolizumab, β_7 Ab or MAdCAM-1 Ab, as indicated. (**B**) Flow-cytometric analysis of $CD69^+/CD103^+$ $CD4^+$ T cell frequency, as in panel A in 6 independent donors. Y-axis indicates the frequency of $CD69^+/CD103^+$ $CD4^+$ T cells. Inclusion of $\alpha_4\beta_7$ antagonists indicated below. (**: $P < 0.01$, two-tailed t test). (**C**) Bar graph representing the average relative frequencies of $CD69^-/CD103^+$ (red), $CD69^+/CD103^+$ (orange), $CD69^-/CD103^-$ (green), and $CD69^+/CD103^-$ (blue) cell populations in the absence or presence of $\alpha_4\beta_7$ antagonists in six independent donors, as indicated. (**D**) Representative flow cytometry dot plot of CCR9 (Y-axis) and CCR5 (X-axis) expression on total $CD4^+$ T cells following costimulation with MAdCAM-1 + RA + TGF-β in the absence or presence of vedolizumab, β_7 Ab or MAdCAM-1 Ab, as indicated. Percent total cells in each quadrant, as indicated.

https://doi.org/10.1371/journal.ppat.1011209.g006

infection, while TGF-β could subsequently drive these cells further toward a T_{RM}-like cell phenotype. To address this issue, we costimulated cells with MAdCAM-1 + RA + TGF-β as described above. VCAM-1 + RA + TGF-β and CD28 Ab + RA + TGF-β were also tested. Sixteen hours prior to the addition of TGF-β, cells were inoculated with an R5-tropic HIV isolate (SF162). Three days after the addition of TGF-β, cells were stained with two HIV p24 mAbs [63], along with anti-CD69 and anti-CD103 (Fig 7A). For most donors, little infection was observed in the absence of a costimulatory ligand. For a small number of donors, we observed infection in the presence of CD3 Ab alone, likely due to a preactivated state of the donor PBMCs. A representative infection of $CD69^+/CD103^+$ T_{RM} cells is provided (Fig 7B), along with results from 10 donors (Fig 7C). To ensure that intracellular p24 staining reflected infection, we employed the R5-antagonist maraviroc (S8 Fig). While CD28 Ab, VCAM-1 and MAdCAM-1 all promoted the formation of T_{RM}-like cells, only MAdCAM-1 + RA costimulation

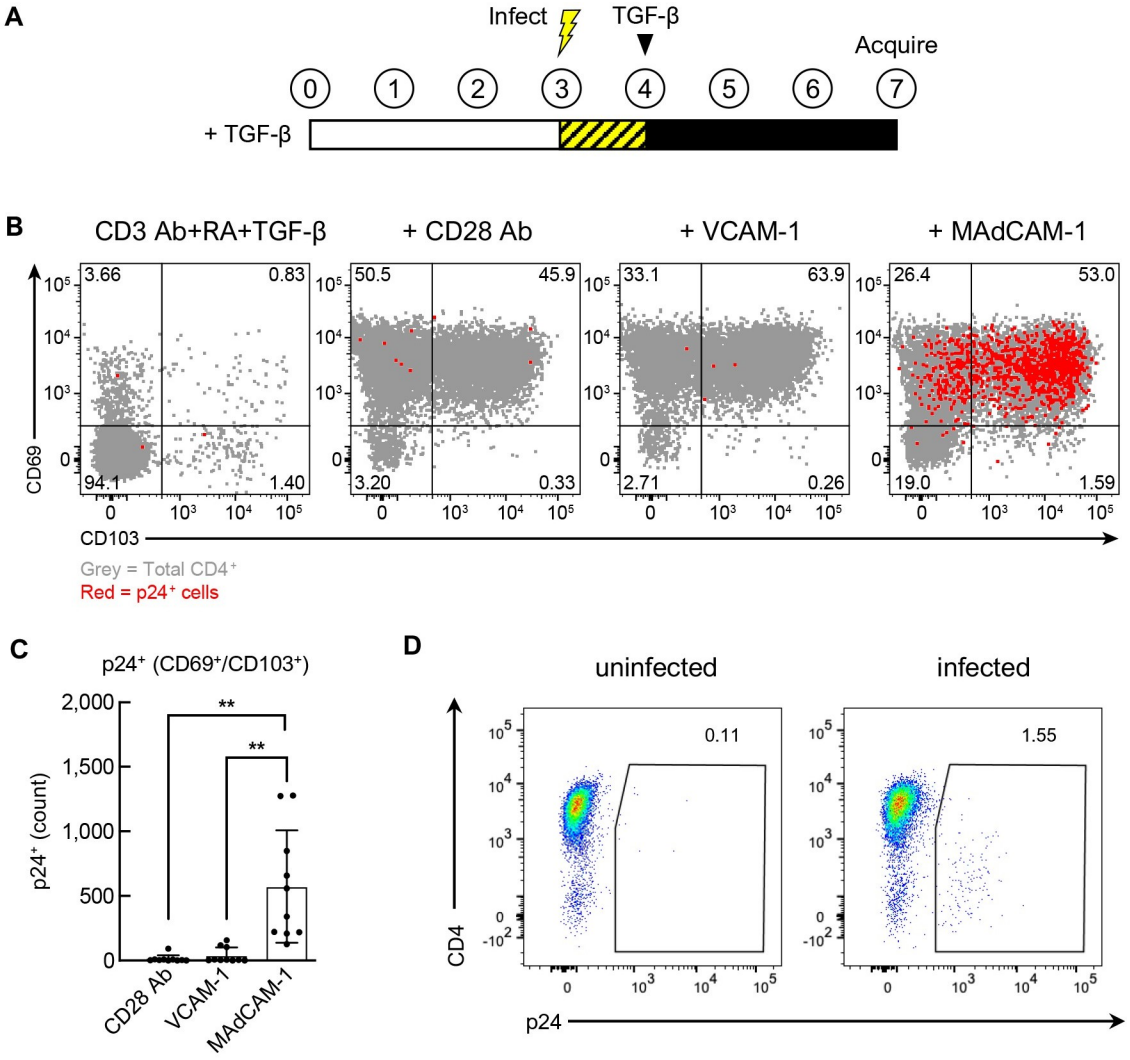

Fig 7. HIV infection following costimulation in the presence of RA and TGF-β. (**A**) Schematic of infection time course. (**B**) Representative flow cytometry dot plot indicating HIV infection of $CD4^+$ T cells costimulated with CD28 Ab, VCAM-1 or MAdCAM-1 in the presence of RA and TGF-β (Y-axis: CD69, X-axis: CD103). $p24^+$ cells shown in red. (**C**) Average number of $p24^+$ cells in the $CD69^+/CD103^+$ population of $CD4^+$ T cells following costimulation as in **B** (n = 10). (**D**) Representative dot plot of CD4 downregulation in $p24^+$ cells. X-axis: p24, Y-axis: CD4. (**: $P < 0.01$, two-tailed t test).

https://doi.org/10.1371/journal.ppat.1011209.g007

consistently supported infection. As expected, CD4 was substantially downregulated on $p24^+$ cells (Fig 7D). These observations are consistent with the capacity of MAdCAM-1, but not VCAM-1 or CD28 Ab, to upregulate CCR5. However, we found that MAdCAM-1 + RA costimulation also supported X4-tropic HIV infection, suggesting that factors other than CCR5 may be involved as well (S8 Fig).

Discussion

The types of cells that contribute to formation of persistent viral reservoirs that form in the first weeks following infection (Fiebig I/II) are a subject of great interest and active investigation [63,64]. Estes and colleagues estimated that >90% of viral RNA positive cells that persist after ART therapy reside in the gut [65,66]. Although the precise identity of these cells is unknown, several studies have demonstrated that $\alpha_4\beta_7^{high}$ memory $CD4^+$ T cells that reside in gut tissues are preferentially infected in Fiebig I/II [67–70]. It is unknown whether T_{RM}s contribute in a significant way to viral reservoirs. Because T_{RM}s can persist in tissues for decades without recirculating, establishing their contribution to viral reservoirs is challenging. Moreover, there is no established way to generate T_{RM}s in vitro. Here we report that stimulating $CD4^+$ T cells with MAdCAM-1 and RA, both of which are associated with $CD4^+$ T cell trafficking to GALT, in combination with TGF-β, a cytokine that suppresses T cell proliferation, drives these cells toward a phenotype consistent with T_{RM}s. These cells express CD103 and CD69, two canonical markers of T_{RM}s, along with $\alpha_4\beta_7$ and CCR9, two receptors that facilitate gut homing. A significant fraction of these T_{RM}-like cells express CCR5. We find that MAdCAM-1 + RA costimulated cells support infection, and the subsequent addition of TGF-β drives the cells to adopt a T_{RM}-like cell phenotype. In this regard, we note that TGF-β can be anti-proliferative for $CD4^+$ T cells. Of note, CCR5-expressing $CD69^+/CD103^+/CD4^+$ T_{RM}s have been identified in rectal mucosa [21]. The model described herein for generating T_{RM}-like cells from peripheral blood $CD4^+$ T cells provides a platform to advance our understanding of the factors that drive differentiation of $CD4^+$ T cells toward a T_{RM} phenotype, as well as the role that this subset of cells might play in the formation of viral reservoirs.

In previous studies, we and others reported that HIV preferentially infects $\alpha_4\beta_7$-expressing $CD4^+/CD45RO^+$ T cells in vitro and in vivo [68,71]. In the course of these studies we determined that, in the presence of RA, signaling by both HIV gp120 and MAdCAM-1 activates cells in a way that supports HIV infection [1,9,11]. Both RA and MAdCAM-1 are modulated in the context of HIV and SIV infection [72,73]. These observations raise the question as to how signaling through $\alpha_4\beta_7$ impacts $CD4^+$ T cell differentiation. In this report we find that MAdCAM-1 provides a distinct costimulatory signal. We found that other costimulatory signals, i.e. VCAM-1 and CD28 Ab, when combined with RA and TGF-β, also generate T_{RM}-like cells. However, VCAM-1 and CD28 Ab do not upregulate CCR5 to the same extent as does MAdCAM-1. Additionally, these cells do not support infection in the same manner as MAdCAM-1.

It is well established that RA upregulates CCR9 and integrin β_7 [45]. We and others have previously noted that RA can also upregulate CCR5 [9,74–77]. In this report, we show that MAdCAM-1 + RA costimulation followed by TGF-β treatment promotes the differentiation of primary $CD4^+$ T cells into $CD69^+/CD103^+$ cells that, for the most part, express either CCR9 or CCR5, with few $CCR9^+/CCR5^+$ cells. We previously reported that CCR5 colocalizes with $\alpha_4\beta_7$ and CD4 on both RA-treated $CD4^+$ T cells and $CD4^+$ T cells isolated from colon biopsies [71]. Although we do not know whether these three receptors work together, it is intriguing to consider that HIV gp120 signals through all three [78].

Although MAdCAM-1 + RA alone was sufficient to induce low levels of $CD69^+/CD103^+$ T_{RM}-like cells, addition of TGF-β increased their frequency in a significant way. We were surprised to find that TGF-β also upregulated CCR5. This effect only occurred in cells treated with RA and most prominently in those costimulated with MAdCAM-1. It is unclear how the combination of MAdCAM-1 and RA predisposes cells to respond to TGF-β in this way. In any case our findings suggest that MAdCAM-1 + RA primes cells to differentiate toward a T_{RM}-like phenotype.

When RA was combined with MAdCAM-1, $CD4^+$ T cell cultures secreted IL-17A and IL-17F. These cells were susceptible to infection, and when TGF-β was added, infected cells could adopt a T_{RM}-like phenotype. In general, TGF-β acts as an immunosuppressive and anti-proliferative cytokine. In mice, the combination of TGF-β and RA promotes $CD4^+$ T cells to differentiate toward a $FoxP3^+$ Treg cell phenotype [49,51]. We can speculate that $CD4^+$ T cells, in gut tissues, stimulated with MAdCAM-1 and RA, when exposed to TGF-β may promote the formation of latent reservoirs. It is unclear why MAdCAM-1 is superior to either VCAM-1 or CD28 Ab with respect to supporting infection. This observation may however help explain why gut tissues generally support very high levels of viral replication during the acute phase of infection.

Several $\alpha_4\beta_7$ or MAdCAM-1 mAb antagonists have been developed to treat IBD. We previously reported that one of these, vedolizumab, inhibited MAdCAM-1-mediated proliferation [9]. Here we show that vedolizumab, anti-integrin β_7 and a MAdCAM-1 Ab, suppressed T_{RM}-like cell differentiation. These antagonists altered the differentiation program of cells in an unusual way. $CD69^-/CD103^+$ cells, which are typically present at a low frequency (average ~ 4%), increased ~2-fold in the presence of these antagonists. Surprisingly, CCR9 and CCR5 expression were not significantly changed. The MAdCAM-1 Ab antagonist did not reduce integrin β_7 expression. Thus, although all three antagonists inhibited T_{RM}-like cell differentiation, their presence resulted in a distinct differentiation pattern not otherwise observed. Further study of the way that these antagonists alter $CD4^+$ T cell differentiation and trafficking may shed light on their mechanism of action in ameliorating the symptoms of IBD.

The capacity of vedolizumab, β_7 Ab and a MAdCAM-1 Ab to suppress the differentiation of T_{RM}-like cells necessarily reduced infection. Such an effect may provide insight into the way that vedolizumab treatment alters infection in vivo [60]. PET/CT imaging of SIV infected macaques treated with ART reveals viral antigen in gut tissues [79]. In a follow-up study, also using PET/CT imaging, we reported that a primatized analogue of vedolizumab reduced viral antigen in the gut without depleting $CD4^+$ cells [59]. In another study, the combination of vedolizumab and a bNAb reduced the frequency of lymphoid aggregates in mesenteric lymph nodes and ileum and delayed viral rebound relative to bNAb treatment alone [80]. Mehandru and colleagues administered vedolizumab to a small number of ART-treated, HIV infected subjects co-afflicted with IBD [60]. Vedolizumab reduced the number of lymphoid aggregates in the GI tract. They noted that these aggregates are important sanctuary sites for establishing and maintaining viral reservoirs [60]. The capacity of $\alpha_4\beta_7$ antagonists to reduce $CD69^+/CD103^+$ T_{RM}-like cell differentiation reported here, along with the above-mentioned in vivo findings, argues for further exploration into the utility of these antagonists in targeting viral reservoirs.

Among the limitations of this study is the incomplete way our in vitro system recapitulates the environment in the gut that drives the formation and maintenance of $CD4^+$ T_{RM}s. This difference limits the longevity of our in vitro derived T_{RM} cells. It will be important to identify soluble factors that extend the lifespan of $CD4^+$ T_{RM} cells. Prlic and colleagues report that $CCR5^+$ T_{RM}s isolated from mucosal tissues can express IL-17 upon restimulation [21]. We did not observe this for the in vitro derived T_{RM}s following restimulation. Thus, further

refinements of this system will be required to increase the similarity between in vitro T_{RM}-like cells and true T_{RM}s present in vivo. Nevertheless, given the challenge of isolating T_{RM}s from humans, the results described herein can potentially help advance our understanding of the role of T_{RM}s in HIV infection. Finally, although we argue that T_{RM}s may contribute to persistent HIV reservoirs, their role in these reservoirs is speculative and remains an open question.

In conclusion, in this report we have shown that MAdCAM-1 costimulation in the presence of RA and TGF-β drives $CD4^+$ T cells toward a $CD69^+/CD103^+$ phenotype that is consistent with T_{RM}s. In the presence of RA and TGF-β, MAdCAM-1 was unique among the costimulatory ligands we tested in inducing CCR5. We speculate that the generation of $CCR5^+$ T_{RM}s may contribute to the pool of persistently infected cells in gut tissues. In this regard we note that penetrance of antiretroviral drugs in the gut can be suboptimal [66,81–83]. Antagonists such as vedolizumab, already approved for the treatment of IBD, suppress MAdCAM-1 costimulation and consequently reduce T_{RM}-like cell formation. These findings will hopefully spur further research into the role of $CD4^+$ T_{RM}s in HIV pathogenesis.

Materials and methods

Human blood samples and primary cell preparation

All primary $CD4^+$ T cells utilized in these studies were isolated from PBMCs collected from healthy donors through a NIH Department of Transfusion Medicine protocol that was approved by the Institutional Review Board of the National Institute of Allergy and Infectious Diseases (NIAID), National Institutes of Health. Informed consent was written and was provided to study participants. PBMCs were isolated from whole blood of healthy donors by Lymphocyte Separation Medium (MP Biomedicals, Santa Clara, CA). Purified $CD4^+$ T cells were derived by negative selection (Stem Cell Technologies, Vancouver, Canada) to >95% purity, as determined by flow cytometry. To ensure that an adequate number of naïve cells were present, purified $CD4^+$ T cells were prescreened by flow cytometry for expression of CD45RO. Cultures with >70% $CD45RO^+$ cells were not used.

Gene expression profiling

RNA extraction methods. $CD4^+$ T cells from 6 donors were subjected to 8 different treatments. All six donors were processed simultaneously to limit error. Approximately 2 x 10^5 human T cells in 100 μl of culture media were lysed with 300μl Trizol LS (Thermofisher Scientific, Waltham, MA), combined with 0.2 volumes of 1-Bromo-3-chloropropane (Sigma, St. Louis, MO), samples mixed, and centrifuged at 16,000 x *g* for 15 min at 4˚C. RNA containing aqueous phase was combined with equal volume of RLT buffer with 1% Beta mercaptoethanol and extracted using AllPrep DNA/RNA 96-well system (Qiagen, Valencia, CA). An additional on-column DNase I treatment was performed during RNA extraction. RNA integrity was assessed using the Agilent 2100 Bioanalyzer using RNA 6000 Pico kit (Agilent Technologies, Santa Clara, CA).

NGS methods. All samples were processed simultaneously. The SMART-Seq v4 Ultra Low Input RNA Kit for Sequencing (Takara Bio, San Jose, CA) was used for cDNA synthesis with an input of 150 pg total RNA. Amplified cDNA was visualized and quantified using BioAnalyzer High Sensitivity chips (Agilent Technologies, Santa Clara, CA). Three hundred picograms of purified cDNA were brought up to 15 uL in volume and sheared on the Covaris LE220 (Covaris Inc., Woburn, MA) using the shearing parameters of PIP 180, 20% DF, 50 bursts/cycle, for 270 seconds with Y-dithering of 5 mm at 20 mm/s. Sequencing ready libraries were generated with 10 uL of sheared cDNA (200 pg) using the ThruPLEX DNA-Seq Library Preparation Kit (Takara Bio, San Jose, CA) and assessed for quality on BioAnalyzer DNA1000

chips (Agilent Technologies, Santa Clara, CA). Libraries were quantified using the Kapa Quant Kit for Illumina sequencing (Kapa Biosystems, Wilmington, MA), normalized to 4 nM, pooled equally, and prepared for sequencing on the NextSeq (Illumina, San Diego, CA) following the user manual guidelines for High Output single read 75 cycle chemistry runs.

RNA-Seq raw data processing and differentially expressed gene selection

The reads of each sample were aligned to human genome GRCh38 by STAR2 software [84], and then followed by HTseq-Count software for read counts of each gene. As a whole group of 96 samples, DESeq2 software package [85] was used to calculate the normalized expression values of genome-wide genes. For each of our 12 treatment-control comparisons (6 different treatments by 2 two time points), we conducted two-tailed t test for p-values, as well as calculated fold changes (FC) for each gene. Differentially expressed gene lists for each comparison were selected with the criteria of $p<0.05$ and FC> absolute (1.50). To condense the data of two time points, final differential expressed gene lists representing each treatment were generated by selecting the more significant time point of the same treatments.

Digital cytometry analysis

A CIBERSORT reference matrix of PBMC cell subgroups was built by combining leukocyte signature genes (LM22) [22] and single cell RNA-Seq based gene expression profiles [23] (see S1 Table). Briefly, the web app Azimuth was used to process scRNA-Seq PBMC datasets. ITGAE gene expression was used as a reference for T_{RM}-like cells. A virtual gene expression profile of T_{RM}-like cells was generated. Bulk RNA-Seq data was then entered into the customized T_{RM} module in order to generate ratios for $CD4^+$ cell subsets including T_{RM}s. For given normalized bulk RNA-Seq expression profiles, CIBERSORT [22] was used to estimate the composition ratios of each cell subgroup based on the reference matrix.

Heatmap visualization

Heatmap of gene expression values of marker genes were generated using either R ggplot2 package or Partek Genomic Suite 7. Bar plots used for presenting the expression changes of the key genes utilized by GraphPad Prism V9 (GraphPad Software, La Jolla, CA). This data has been deposited in the GSEA data base, under accession # GSE221434. You can access this data at https://www.ncbi.nlm.nih.gov/geo/query/acc.cgi?acc=GSE221434

Customized gene set enrichment analysis

The reference marker gene sets relevant to T_{RM}, T_{EM} and T_{CM} were derived from scRNA-Seq PBMC datasets [22] using FindMarkers function provided in the Seurat 4.0 package [23]. The reference marker gene sets were also manually annotated from relevant publication [29]. In addition, some immunologically relevant pathways were also collected from MSigDB [86]. These collections served as customized reference gene signatures for the gene functional enrichment analysis using Broad Institute's Gene Set Enrichment Analysis (GSEA) software 4.1.0. [24].

RT-qPCR

Key biological findings from the RNA-Seq were validated by RT-qPCR. Validation analysis was performed in a subset of RNA-Seq samples. The validation sample-set consisted of day 2 samples with RA treatment in 3 donors. S4 Table lists 3 selected biologically relevant genes and one house-keeping gene for RT-qPCR validation. Primer Express software for Real-Time

PCR v3.0.1 (Life science technologies, Carlsbad, CA) was used to design primer sets. Selected primers and probes spanned two conserved exons with the minimum intron length of 1kb that do not cross-hybridize with paralogous gene sequences. Probe and primer sets were ordered from Biosearch Technologies (Biosearch technologies, Novato, CA).

Template cDNAs were synthesized using SuperScript VILO cDNA synthesis kit (Thermo-Scientific, Waltham, MA) and were purified using the QIAquick 96 PCR Purification Kit (Qiagen, Valencia, CA). The Invitrogen Express qPCR supermix with premixed ROX (Invitrogen, Carlsbad, CA) reactions were carried out in 20 uL reactions with 1X RT-PCR buffer, 400 nM of forward and reverse primers, 120 nM of fluorescent TaqMan probe(s). The qPCR reactions were carried out at 50˚C for 2 min, 95˚C for 2 min, and 55 cycles of 95˚C for 15 sec and 60˚C for 1 minute. Data was analyzed using Applied Biosystems 7900HT Sequence Detection Systems version 2.4.1 software (Life technologies, Carlsbad, CA). Normalized NGS read count values were used for correlation with qPCR data. The correlation analysis was carried out using Prism and Spearman correlations were calculated between qPCR and NGS read count values.

Cytokine immunoassays

Cytokine concentrations in culture supernatants from 3 independent donors were determined with a bead-based immunoassay (Luminex, Human Th17 multiplex kit (HTH17MG-14K-PX25). Culture supernatants were collected at 72 hrs (MAdCAM-1) or 96 hrs (cV2). Data collection was carried out with a Luminex 200 xMAP instrument following the manufacturer's instructions.

Costimulation assays and tissue culture reagents

MAdCAM-1-Ig and VCAM-Ig were obtained from R&D Systems (Minneapolis, MN). CD28 Ab was purchased from Invitrogen (Carlsbad, CA). Costimulatory ligands were biotinylated per the manufacturer's instructions using a LYNX Rapid Plus Biotin (Type 2) Antibody Conjugation Kit (Bio-Rad, Hercules CA). Costimulation assays were carried out as previously described [11] with several modifications. 96-well flat bottom cell culture-treated plates (Corning, Corning, NY) were first pre-coated with 50 ng of CD3 Ab (clone OKT3) (eBioscience, San Diego, CA) at 4˚C for 2 hours, followed by 200 ng of NeutrAvidin (Invitrogen, Carlsbad, CA) at 4˚C overnight in 100 μl HBS. 200 ng of biotinylated costimulatory ligand was then added for 1 hour at 37˚C. 200,000 purified $CD4^+$ T cells were then added to coated wells and cultured in complete RPMI 1640 medium with 2% L-glutamine-penicillin-streptomycin (Gibco Laboratories, Gaithersburg, MD) and 10% FBS (Gibco Laboratories, Gaithersburg, MD) (1 x 10^6 cells/ml) at 37˚C, 5% CO_2. In some cultures, 10 nM all-trans retinoic acid (Sigma-Aldrich, St. Louis MO) was included. On day 4, cultures were replaced with fresh complete media. In some cultures, TGF-β (1 ng/ml) was also added on day 4. On day 7, cells were harvested and analyzed by flow cytometry using FlowJo software. In some experiments, 2 μg/ml of $\alpha_4\beta_7$ mAb antagonists (vedolizumab, β_7 Ab clone FIB504, MAdCAM-1 Ab clone 314G8) or a control mAb were added on day 4 along with TGF-β.

Antibodies and flow cytometry

Antibody staining, carried out in 2% FBS in 1X PBS, employed standard protocols. mAbs utilized for flow cytometry are listed in S5 Table. For intracellular FoxP3 staining, cells were first stained for surface markers and then permeabilized using a FoxP3 staining buffer (eBioscience, San Diego, CA). Data was collected on a FACSCanto II (BD Biosciences, San Diego, CA) and analyzed using FlowJo. Statistical significance was determined with Prism. Two-tailed t tests were applied, and p values reported.

Viral infection assay

A molecular clone of HIV SF162 (R5-tropic, subtype B) (accession number EU123924) was utilized in all infections. This stock was produced by transient transfection of 293T cells and then briefly passaged through PBMCs. For infection, 0.2 μl of 0.29 ng/μl (p24) was added on day 3 following MAdCAM-1, VCAM-1, or CD28 Ab costimulation. After 18 hrs, cells were rinsed 3X and replaced with fresh media. On day 7 post stimulation, cells were stained with Live/Dead Aqua (Invitrogen, Carlsbad, CA), fixed and permeabilized (Cytofix/Cytoperm, BD Biosciences, San Diego, CA) and stained with two intracellular anti p24 Gag antigen mAbs [63]. Cells were analyzed by flow cytometry and infection was determined by the percentage of cells double positive for p24 Gag antigen.

Supporting information

S1 Fig. Validation of RNA-Seq results by RT-qPCR and TF modulation. RT-qPCR was performed on RNA derived from CD4$^+$ T cells costimulated with CD28 Ab, MAdCAM-1 and cV2, all in the presence of RA (n = 3). Primers and probes specific to CCR7 (left), SELL (middle) and S1PR1 (right) we employed. Values were normalized to the housekeeping gene TAF1D, and relative units (RU) reported. Error bars indicate standard deviation. (**B**) The T_{RM} lineage signal translation pathway following MAdCAM-1 + RA treatment is shown. TF genes in the pathway are depicted illustrated as ovals, with a four-color scheme of red, pink, green, and white, which respectively represent up-regulation ($>$ 1.5 fold), moderate up-regulation (1.25–1.5 fold), down-regulation ($<$ -1.5 fold), and no significant changes. Relevant surface receptors are depicted as rectangles.
(TIF)

S2 Fig. Cytokine secretion in response to MAdCAM-1 + RA costimulation. Bead based immunoassay of cytokines in culture supernatants following CD3 Ab + MAdCAM-1 (white bar) or CD3 Ab + MAdCAM-1 + RA (black bar) costimulation of CD4$^+$ T cells. Average cytokine concentration (pg/ml) from 3 independent donors. Error bars indicate standard deviation. Only the analytes that yielded signals above the limit of detection are shown.
(TIF)

S3 Fig. Cytokine secretion in response to cV2 + RA costimulation. Bead based immunoassay of cytokines in culture supernatants following CD3 Ab + cV2 (white bar) or CD3 Ab + cV2 + RA (black bar) costimulation of CD4$^+$ T cells. Average cytokine concentration (pg/ml) from 3 independent donors. Error bars indicate standard deviation. Only the analytes that yielded signals above the limit of detection are shown.
(TIF)

S4 Fig. Co-expression of $\alpha_4\beta_7$ and $\alpha_E\beta_7$ on CD4$^+$ T_{RM}s in the presence of TGF-β. (**A**) Flow-cytometric analysis of $\alpha_4\beta_7$ expression on total CD4$^+$ T cells without any stimulation or with CD3 Ab + RA, CD3 Ab + MAdCAM-1 + RA, CD3 Ab + VCAM-1 + RA, or CD3 Ab + CD28 Ab + RA in the absence or presence of TGF-β as indicated. (**B**) $\alpha_4\beta_7$ expression on CD69$^+$/$\alpha_E\beta_7^+$ CD4$^+$ T cells following CD3 Ab + MAdCAM-1, CD3 Ab + VCAM-1, or CD3 Ab + CD28 Ab, as indicated (n = 6).
(TIF)

S5 Fig. Expression of CCR5 on MAdCAM-1 + RA stimulated cells. Representative flow cytometry dot plot of CCR5 expression within the CD69$^+$/CD103$^+$ population are shown. Cells stimulated with MAdCAM-1 (left), VCAM-1 (middle), and CD28 Ab (right) are shown.

Y-axis: FSC-A, X-axis: CCR5.
(TIF)

S6 Fig. CXCR3 and CCR6 expression on MAdCAM-1 costimulated cells. (**A**) Representative flow cytometric dot plot of MAdCAM-1 + RA + TGF-β treated cells. $CD69^+/CD103^+$ cells (left) were stained with CXCR3 (Y-axis) and CCR6 (X-axis). (**B**) CXCR3 (left) and CCR6 (right) expression in 5 independent donors.
(TIF)

S7 Fig. CCR9, CCR5, and integrin β_7 expression in the presence of $\alpha_4\beta_7$ antagonists. Flow-cytometric analysis of (**A**) CCR9 (n = 5), (**B**) CCR5 (n = 5), (**C**) integrin β_7 (n = 3) in the total $CD4^+$ T cell population following MAdCAM-1 + RA + TGF-β costimulation in the absence or presence of vedolizumab, β_7 Ab, or MAdCAM-1 Ab, as indicated.
(TIF)

S8 Fig. Intracellular p24 staining of R5 and X4-tropic isolates of HIV in the presence of Marviroc. (**A**) Representative dot plot of an R5 tropic isolate (SF162) (upper row) and an X4-tropic isolate (NL4-3) (lower row) alone (left) or in the presence of maraviroc (middle) or T20 (right) following MAdCAM-1 + RA + TGF-β treatment. Cells shown are $CD69^+/CD103^+$. (**B**) p24 staining, as in A for 3 donors for SF162 (left) and NL4-3 (right).
(TIF)

S1 Table. CIBERSORT Reference module of $CD4^+$ cell subtypes following MAdCAM-1 + RA costimulation.
(DOCX)

S2 Table. GSEA analysis results of CD3 Ab + MAdCAM-1 + RA and CD3 Ab + CD28 Ab + RA treatment groups.
(DOCX)

S3 Table. T_{RM} knowledge database.
(DOCX)

S4 Table. RT-qPCR oligo sequences.
(DOCX)

S5 Table. Flow cytometry antibodies.
(DOCX)

Acknowledgments

The authors would like to thank Aftab Ansari for the gift of MAdCAM-1 Ab clone 314G8. We would also like to thank Elena Martinelli, Lyle McKinnon and Alexandra Schuetz for discussion and advice, and Aaron Weddle for assistance with figure preparation.

Author Contributions

Conceptualization: Sinmanus Vimonpatranon, Livia R. Goes, James Arthos, Claudia Cicala.

Formal analysis: Sinmanus Vimonpatranon, Livia R. Goes, Dawei Huang, Andrew Jiang, Cindy Huang, Joyce Zhou, James Arthos, Claudia Cicala.

Investigation: Sinmanus Vimonpatranon, Livia R. Goes, Amanda Chan, Isabella Licavoli, Jordan McMurry, Samuel R. Wertz, Cindy Huang, Joyce Zhou, Alexandre Girard, Danlan

Wei, Il Young Hwang, Kishore Kanakabandi, Kimmo Virtaneva, Stacy Ricklefs, Benjamin P. Darwitz.

Methodology: Anush Arakelyan, Dawei Huang, Andrew Jiang, Craig Martens, Claudia Cicala.

Supervision: Donald Van Ryk, Danlan Wei, James Arthos, Claudia Cicala.

Writing – original draft: Sinmanus Vimonpatranon, Livia R. Goes, James Arthos, Claudia Cicala.

Writing – review & editing: Anush Arakelyan, Dawei Huang, Jason Yolitz, Donald Van Ryk, Craig Martens, Marcelo A. Soares, Kovit Pattanapanyasat, Anthony S. Fauci, James Arthos, Claudia Cicala.

References

1. Arthos J, Cicala C, Nawaz F, Byrareddy SN, Villinger F, Santangelo PJ, et al. The Role of Integrin alpha4beta7 in HIV Pathogenesis and Treatment. Curr HIV/AIDS Rep. 2018; 15(2):127–35.
2. Le Hingrat Q, Sereti I, Landay AL, Pandrea I, Apetrei C. The Hitchhiker Guide to CD4(+) T-Cell Depletion in Lentiviral Infection. A Critical Review of the Dynamics of the CD4(+) T Cells in SIV and HIV Infection. Front Immunol. 2021; 12:695674. https://doi.org/10.3389/fimmu.2021.695674 PMID: 34367156
3. Mehandru S, Poles MA, Tenner-racz K, Horowitz A, Hurley A, Hogan C, et al. Primary HIV-1 Infection Is Associated with Preferential Depletion of CD4+ T Lymphocytes from Effector Sites in the Gastrointestinal Tract. The Journal of Experimental Medicine. 2004; 200(6):761–70. https://doi.org/10.1084/jem.20041196 PMID: 15365095
4. Mehandru S, Poles MA, Tenner-Racz K, Jean-Pierre P, Manuelli V, Lopez P, et al. Lack of mucosal immune reconstitution during prolonged treatment of acute and early HIV-1 infection. PLoS Med. 2006; 3(12):e484. https://doi.org/10.1371/journal.pmed.0030484 PMID: 17147468
5. Mehandru S, Poles MA, Tenner-Racz K, Manuelli V, Jean-Pierre P, Lopez P, et al. Mechanisms of gastrointestinal CD4+ T-cell depletion during acute and early human immunodeficiency virus type 1 infection. J Virol. 2007; 81(2):599–612. https://doi.org/10.1128/JVI.01739-06 PMID: 17065209
6. Tanaka Y. T cell integrin activation by chemokines in inflammation. Arch Immunol Ther Exp (Warsz). 2000; 48(6):443–50. PMID: 11197597
7. Tanaka Y. Integrin activation by chemokines: relevance to inflammatory adhesion cascade during T cell migration. Histol Histopathol. 2000; 15(4):1169–76. https://doi.org/10.14670/HH-15.1169 PMID: 11005242
8. Lehnert K, Print CG, Yang Y, Krissansen GW. MAdCAM-1 costimulates T cell proliferation exclusively through integrin alpha4beta7, whereas VCAM-1 and CS-1 peptide use alpha4beta1: evidence for "remote" costimulation and induction of hyperresponsiveness to B7 molecules. Eur J Immunol. 1998; 28(11):3605–15. https://doi.org/10.1002/(SICI)1521-4141(199811)28:11<3605::AID-IMMU3605>3.0.CO;2-J PMID: 9842903
9. Nawaz F, Goes LR, Ray JC, Olowojesiku R, Sajani A, Ansari AA, et al. MAdCAM costimulation through Integrin-alpha4beta7 promotes HIV replication. Mucosal Immunol. 2018.
10. Arthos J, Cicala C, Martinelli E, Macleod K, Van Ryk D, Wei D, et al. HIV-1 envelope protein binds to and signals through integrin alpha4beta7, the gut mucosal homing receptor for peripheral T cells. Nat Immunol. 2008; 9(3):301–9. https://doi.org/10.1038/ni1566 PMID: 18264102
11. Goes LR, Sajani A, Sivro A, Olowojesiku R, Ray JC, Perrone I, et al. The V2 loop of HIV gp120 delivers costimulatory signals to CD4(+) T cells through Integrin alpha4beta7 and promotes cellular activation and infection. Proc Natl Acad Sci U S A. 2020; 117(51):32566–73.
12. Lertjuthaporn S, Cicala C, Van Ryk D, Liu M, Yolitz J, Wei D, et al. Select gp120 V2 domain specific antibodies derived from HIV and SIV infection and vaccination inhibit gp120 binding to alpha4beta7. PLoS Pathog. 2018; 14(8):e1007278.
13. Faria AMC, Reis BS, Mucida D. Tissue adaptation: Implications for gut immunity and tolerance. J Exp Med. 2017; 214(5):1211–26. https://doi.org/10.1084/jem.20162014 PMID: 28432200
14. Kumar BV, Kratchmarov R, Miron M, Carpenter DJ, Senda T, Lerner H, et al. Functional heterogeneity of human tissue-resident memory T cells based on dye efflux capacities. JCI Insight. 2018; 3(22). https://doi.org/10.1172/jci.insight.123568 PMID: 30429372

15. Kumar BV, Ma W, Miron M, Granot T, Guyer RS, Carpenter DJ, et al. Human Tissue-Resident Memory T Cells Are Defined by Core Transcriptional and Functional Signatures in Lymphoid and Mucosal Sites. Cell Rep. 2017; 20(12):2921–34. https://doi.org/10.1016/j.celrep.2017.08.078 PMID: 28930685

16. Turner DL, Farber DL. Mucosal resident memory CD4 T cells in protection and immunopathology. Front Immunol. 2014; 5:331. https://doi.org/10.3389/fimmu.2014.00331 PMID: 25071787

17. Cantero-Perez J, Grau-Exposito J, Serra-Peinado C, Rosero DA, Luque-Ballesteros L, Astorga-Gamaza A, et al. Resident memory T cells are a cellular reservoir for HIV in the cervical mucosa. Nat Commun. 2019; 10(1):4739. https://doi.org/10.1038/s41467-019-12732-2 PMID: 31628331

18. Couturier J, Suliburk JW, Brown JM, Luke DJ, Agarwal N, Yu X, et al. Human adipose tissue as a reservoir for memory CD4+ T cells and HIV. AIDS. 2015; 29(6):667–74. https://doi.org/10.1097/QAD.0000000000000599 PMID: 25849830

19. Hsiao F, Frouard J, Gramatica A, Xie G, Telwatte S, Lee GQ, et al. Tissue memory CD4+ T cells expressing IL-7 receptor-alpha (CD127) preferentially support latent HIV-1 infection. PLoS Pathog. 2020; 16(4):e1008450. https://doi.org/10.1371/journal.ppat.1008450 PMID: 32353080

20. Neidleman J, Luo X, Frouard J, Xie G, Hsiao F, Ma T, et al. Phenotypic analysis of the unstimulated in vivo HIV CD4 T cell reservoir. Elife. 2020;9. https://doi.org/10.7554/eLife.60933 PMID: 32990219

21. Woodward Davis AS, Roozen HN, Dufort MJ, DeBerg HA, Delaney MA, Mair F, et al. The human tissue-resident CCR5(+) T cell compartment maintains protective and functional properties during inflammation. Sci Transl Med. 2019; 11(521). https://doi.org/10.1126/scitranslmed.aaw8718 PMID: 31801887

22. Newman AM, Liu CL, Green MR, Gentles AJ, Feng W, Xu Y, et al. Robust enumeration of cell subsets from tissue expression profiles. Nat Methods. 2015; 12(5):453–7. https://doi.org/10.1038/nmeth.3337 PMID: 25822800

23. Stuart T, Butler A, Hoffman P, Hafemeister C, Papalexi E, Mauck WM, 3rd, et al. Comprehensive Integration of Single-Cell Data. Cell. 2019; 177(7):1888–902 e21. https://doi.org/10.1016/j.cell.2019.05.031 PMID: 31178118

24. Subramanian A, Tamayo P, Mootha VK, Mukherjee S, Ebert BL, Gillette MA, et al. Gene set enrichment analysis: a knowledge-based approach for interpreting genome-wide expression profiles. Proc Natl Acad Sci U S A. 2005; 102(43):15545–50. https://doi.org/10.1073/pnas.0506580102 PMID: 16199517

25. Cibrian D, Sanchez-Madrid F. CD69: from activation marker to metabolic gatekeeper. Eur J Immunol. 2017; 47(6):946–53. https://doi.org/10.1002/eji.201646837 PMID: 28475283

26. FitzPatrick MEB, Provine NM, Garner LC, Powell K, Amini A, Irwin SL, et al. Human intestinal tissue-resident memory T cells comprise transcriptionally and functionally distinct subsets. Cell Rep. 2021; 34 (3):108661.

27. Hardenberg JB, Braun A, Schon MP. A Yin and Yang in Epithelial Immunology: The Roles of the alphaE (CD103)beta7 Integrin in T Cells. J Invest Dermatol. 2018; 138(1):23–31.

28. Gorfu G, Rivera-Nieves J, Ley K. Role of beta7 integrins in intestinal lymphocyte homing and retention. Curr Mol Med. 2009; 9(7):836–50. https://doi.org/10.2174/156652409789105525 PMID: 19860663

29. Amsen D, van Gisbergen K, Hombrink P, van Lier RAW. Tissue-resident memory T cells at the center of immunity to solid tumors. Nat Immunol. 2018; 19(6):538–46. https://doi.org/10.1038/s41590-018-0114-2 PMID: 29777219

30. Boddupalli CS, Nair S, Gray SM, Nowyhed HN, Verma R, Gibson JA, et al. ABC transporters and NR4A1 identify a quiescent subset of tissue-resident memory T cells. J Clin Invest. 2016; 126 (10):3905–16. https://doi.org/10.1172/JCI85329 PMID: 27617863

31. Laidlaw BJ, Zhang N, Marshall HD, Staron MM, Guan T, Hu Y, et al. CD4+ T cell help guides formation of CD103+ lung-resident memory CD8+ T cells during influenza viral infection. Immunity. 2014; 41 (4):633–45. https://doi.org/10.1016/j.immuni.2014.09.007 PMID: 25308332

32. Mackay LK, Wynne-Jones E, Freestone D, Pellicci DG, Mielke LA, Newman DM, et al. T-box Transcription Factors Combine with the Cytokines TGF-beta and IL-15 to Control Tissue-Resident Memory T Cell Fate. Immunity. 2015; 43(6):1101–11.

33. Ramirez JM, Brembilla NC, Sorg O, Chicheportiche R, Matthes T, Dayer JM, et al. Activation of the aryl hydrocarbon receptor reveals distinct requirements for IL-22 and IL-17 production by human T helper cells. Eur J Immunol. 2010; 40(9):2450–9. https://doi.org/10.1002/eji.201040461 PMID: 20706985

34. Intlekofer AM, Takemoto N, Wherry EJ, Longworth SA, Northrup JT, Palanivel VR, et al. Effector and memory CD8+ T cell fate coupled by T-bet and eomesodermin. Nat Immunol. 2005; 6(12):1236–44. https://doi.org/10.1038/ni1268 PMID: 16273099

35. Dhodapkar MV, Dhodapkar KM. Tissue-resident memory-like T cells in tumor immunity: Clinical implications. Semin Immunol. 2020; 49:101415. https://doi.org/10.1016/j.smim.2020.101415 PMID: 33011063

36. Mueller SN, Mackay LK. Tissue-resident memory T cells: local specialists in immune defence. Nat Rev Immunol. 2016; 16(2):79–89. https://doi.org/10.1038/nri.2015.3 PMID: 26688350

37. Wu J, Madi A, Mieg A, Hotz-Wagenblatt A, Weisshaar N, Ma S, et al. T Cell Factor 1 Suppresses CD103+ Lung Tissue-Resident Memory T Cell Development. Cell Rep. 2020; 31(1):107484. https://doi.org/10.1016/j.celrep.2020.03.048 PMID: 32268106

38. Skon CN, Lee JY, Anderson KG, Masopust D, Hogquist KA, Jameson SC. Transcriptional downregulation of S1pr1 is required for the establishment of resident memory CD8+ T cells. Nat Immunol. 2013; 14 (12):1285–93. https://doi.org/10.1038/ni.2745 PMID: 24162775

39. Aschenbrenner D, Foglierini M, Jarrossay D, Hu D, Weiner HL, Kuchroo VK, et al. An immunoregulatory and tissue-residency program modulated by c-MAF in human TH17 cells. Nat Immunol. 2018; 19 (10):1126–36. https://doi.org/10.1038/s41590-018-0200-5 PMID: 30201991

40. Korn T, Bettelli E, Oukka M, Kuchroo VK. IL-17 and Th17 Cells. Annu Rev Immunol. 2009; 27:485–517. https://doi.org/10.1146/annurev.immunol.021908.132710 PMID: 19132915

41. Sheridan BS, Lefrancois L. Regional and mucosal memory T cells. Nat Immunol. 2011; 12(6):485–91. https://doi.org/10.1038/ni.2029 PMID: 21739671

42. Shimizu Y, van Seventer GA, Horgan KJ, Shaw S. Costimulation of proliferative responses of resting CD4+ T cells by the interaction of VLA-4 and VLA-5 with fibronectin or VLA-6 with laminin. J Immunol. 1990; 145(1):59–67. PMID: 1972721

43. Shimizu Y, van Seventer GA, Horgan KJ, Shaw S. Roles of adhesion molecules in T-cell recognition: fundamental similarities between four integrins on resting human T cells (LFA-1, VLA-4, VLA-5, VLA-6) in expression, binding, and costimulation. Immunol Rev. 1990; 114:109–43. https://doi.org/10.1111/j.1600-065x.1990.tb00563.x PMID: 2196219

44. Zhang N, Bevan MJ. Transforming growth factor-beta signaling controls the formation and maintenance of gut-resident memory T cells by regulating migration and retention. Immunity. 2013; 39(4):687–96.

45. Iwata M, Hirakiyama A, Eshima Y, Kagechika H, Kato C, Song SY. Retinoic acid imprints gut-homing specificity on T cells. Immunity. 2004; 21(4):527–38. https://doi.org/10.1016/j.immuni.2004.08.011 PMID: 15485630

46. Fu H, Jangani M, Parmar A, Wang G, Coe D, Spear S, et al. A Subset of CCL25-Induced Gut-Homing T Cells Affects Intestinal Immunity to Infection and Cancer. Front Immunol. 2019; 10:271. https://doi.org/10.3389/fimmu.2019.00271 PMID: 30863398

47. Shaw GM, Hunter E. HIV transmission. Cold Spring Harb Perspect Med. 2012; 2(11). https://doi.org/10.1101/cshperspect.a006965 PMID: 23043157

48. Mucida D, Cheroutre H. TGFbeta and retinoic acid intersect in immune-regulation. Cell Adh Migr. 2007; 1(3):142–4. https://doi.org/10.4161/cam.1.3.5062 PMID: 19262136

49. Mucida D, Park Y, Cheroutre H. From the diet to the nucleus: vitamin A and TGF-beta join efforts at the mucosal interface of the intestine. Semin Immunol. 2009; 21(1):14–21. https://doi.org/10.1016/j.smim.2008.08.001 PMID: 18809338

50. Mucida D, Park Y, Kim G, Turovskaya O, Scott I, Kronenberg M, et al. Reciprocal TH17 and regulatory T cell differentiation mediated by retinoic acid. Science. 2007; 317(5835):256–60. https://doi.org/10.1126/science.1145697 PMID: 17569825

51. Mucida D, Pino-Lagos K, Kim G, Nowak E, Benson MJ, Kronenberg M, et al. Retinoic acid can directly promote TGF-beta-mediated Foxp3(+) Treg cell conversion of naive T cells. Immunity. 2009; 30 (4):471–2; author reply 2–3. https://doi.org/10.1016/j.immuni.2009.03.008 PMID: 19371709

52. Cosmi L, Cimaz R, Maggi L, Santarlasci V, Capone M, Borriello F, et al. Evidence of the transient nature of the Th17 phenotype of CD4+CD161+ T cells in the synovial fluid of patients with juvenile idiopathic arthritis. Arthritis Rheum. 2011; 63(8):2504–15. https://doi.org/10.1002/art.30332 PMID: 21381000

53. Geginat J, Paroni M, Maglie S, Alfen JS, Kastirr I, Gruarin P, et al. Plasticity of human CD4 T cell subsets. Front Immunol. 2014; 5:630. https://doi.org/10.3389/fimmu.2014.00630 PMID: 25566245

54. Behr FM, Chuwonpad A, Stark R, van Gisbergen K. Armed and Ready: Transcriptional Regulation of Tissue-Resident Memory CD8 T Cells. Front Immunol. 2018; 9:1770. https://doi.org/10.3389/fimmu.2018.01770 PMID: 30131803

55. Battat R, Dulai PS, Jairath V, Vande Casteele N. A product review of vedolizumab in inflammatory bowel disease. Hum Vaccin Immunother. 2019; 15(10):2482–90. https://doi.org/10.1080/21645515.2019.1591139 PMID: 30897022

56. Tang MT, Keir ME, Erickson R, Stefanich EG, Fuh FK, Ramirez-Montagut T, et al. Review article: non-clinical and clinical pharmacology, pharmacokinetics and pharmacodynamics of etrolizumab, an anti-beta7 integrin therapy for inflammatory bowel disease. Aliment Pharmacol Ther. 2018; 47(11):1440–52.

57. D'Haens GR, Reinisch W, Lee SD, Tarabar D, Louis E, Klopocka M, et al. Long-Term Safety and Efficacy of the Anti-Mucosal Addressin Cell Adhesion Molecule-1 Monoclonal Antibody Ontamalimab (SHP647) for the Treatment of Crohn's Disease: The OPERA II Study. Inflamm Bowel Dis. 2021.

58. Reinisch W, Sandborn WJ, Danese S, Hebuterne X, Klopocka M, Tarabar D, et al. Long-term Safety and Efficacy of the Anti-MAdCAM-1 Monoclonal Antibody Ontamalimab [SHP647] for the Treatment of Ulcerative Colitis: The Open-label Study TURANDOT II. J Crohns Colitis. 2021; 15(6):938–49. https://doi.org/10.1093/ecco-jcc/jjab023 PMID: 33599720

59. Santangelo PJ, Cicala C, Byrareddy SN, Ortiz KT, Little D, Lindsay KE, et al. Early treatment of SIV+ macaques with an alpha4beta7 mAb alters virus distribution and preserves CD4(+) T cells in later stages of infection. Mucosal Immunol. 2018; 11(3):932–46.

60. Uzzan M, Tokuyama M, Rosenstein AK, Tomescu C, SahBandar IN, Ko HM, et al. Anti-alpha4beta7 therapy targets lymphoid aggregates in the gastrointestinal tract of HIV-1-infected individuals. Sci Transl Med. 2018; 10(461).

61. DeBerg HA, Konecny AJ, Shows DM, Lord JD. MAdCAM-1 Costimulates T Cells through Integrin alpha4beta7 to Cause Gene Expression Events Resembling Costimulation through CD28. Immunohorizons. 2022; 6(3):211–23.

62. Leung E, Lehnert KB, Kanwar JR, Yang Y, Mon Y, McNeil HP, et al. Bioassay detects soluble MAdCAM-1 in body fluids. Immunol Cell Biol. 2004; 82(4):400–9. https://doi.org/10.1111/j.0818-9641.2004.01247.x PMID: 15283850

63. Pardons M, Baxter AE, Massanella M, Pagliuzza A, Fromentin R, Dufour C, et al. Single-cell characterization and quantification of translation-competent viral reservoirs in treated and untreated HIV infection. PLoS Pathog. 2019; 15(2):e1007619. https://doi.org/10.1371/journal.ppat.1007619 PMID: 30811499

64. Kazer SW, Walker BD, Shalek AK. Evolution and Diversity of Immune Responses during Acute HIV Infection. Immunity. 2020; 53(5):908–24. https://doi.org/10.1016/j.immuni.2020.10.015 PMID: 33207216

65. Busman-Sahay K, Starke CE, Nekorchuk MD, Estes JD. Eliminating HIV reservoirs for a cure: the issue is in the tissue. Curr Opin HIV AIDS. 2021; 16(4):200–8. https://doi.org/10.1097/COH.0000000000000688 PMID: 34039843

66. Estes JD, Kityo C, Ssali F, Swainson L, Makamdop KN, Del Prete GQ, et al. Defining total-body AIDS-virus burden with implications for curative strategies. Nat Med. 2017; 23(11):1271–6. https://doi.org/10.1038/nm.4411 PMID: 28967921

67. Calenda G, Villegas G, Reis A, Millen L, Barnable P, Mamkina L, et al. Mucosal Susceptibility to Human Immunodeficiency Virus Infection in the Proliferative and Secretory Phases of the Menstrual Cycle. AIDS Res Hum Retroviruses. 2019; 35(3):335–47. https://doi.org/10.1089/AID.2018.0154 PMID: 30600686

68. Sivro A, Schuetz A, Sheward D, Joag V, Yegorov S, Liebenberg LJ, et al. Integrin alpha4beta7 expression on peripheral blood CD4(+) T cells predicts HIV acquisition and disease progression outcomes. Sci Transl Med. 2018; 10(425).

69. Tokarev A, McKinnon LR, Pagliuzza A, Sivro A, Omole TE, Kroon E, et al. Preferential Infection of alpha4beta7+ Memory CD4+ T Cells During Early Acute Human Immunodeficiency Virus Type 1 Infection. Clin Infect Dis. 2020; 71(11):e735–e43.

70. Vaccari M, Gordon SN, Fourati S, Schifanella L, Liyanage NP, Cameron M, et al. Adjuvant-dependent innate and adaptive immune signatures of risk of SIV acquisition. Nature Medicine. 2016; 22:762–70.

71. Cicala C, Martinelli E, McNally JP, Goode DJ, Gopaul R, Hiatt J, et al. The integrin alpha4beta7 forms a complex with cell-surface CD4 and defines a T-cell subset that is highly susceptible to infection by HIV-1. Proc Natl Acad Sci U S A. 2009; 106(49):20877–82. https://doi.org/10.1073/pnas.0911796106 PMID: 19933330

72. Kasarpalkar NJ, Bhowmick S, Patel V, Savardekar L, Agrawal S, Shastri J, et al. Frequency of Effector Memory Cells Expressing Integrin alpha(4)beta(7) Is Associated With TGF-beta1 Levels in Therapy Naive HIV Infected Women With Low CD4(+) T Cell Count. Front Immunol. 2021; 12:651122.

73. Sidell N, Kane MA. Actions of Retinoic Acid in the Pathophysiology of HIV Infection. Nutrients. 2022; 14(8). https://doi.org/10.3390/nu14081611 PMID: 35458172

74. Monteiro P, Gosselin A, Wacleche VS, El-Far M, Said EA, Kared H, et al. Memory CCR6+CD4+ T cells are preferential targets for productive HIV type 1 infection regardless of their expression of integrin beta7. J Immunol. 2011; 186(8):4618–30.

75. Planas D, Zhang Y, Monteiro P, Goulet JP, Gosselin A, Grandvaux N, et al. HIV-1 selectively targets gut-homing CCR6+CD4+ T cells via mTOR-dependent mechanisms. JCI Insight. 2017; 2(15). https://doi.org/10.1172/jci.insight.93230 PMID: 28768913

76. Renault C, Veyrenche N, Mennechet F, Bedin AS, Routy JP, Van de Perre P, et al. Th17 CD4+ T-Cell as a Preferential Target for HIV Reservoirs. Front Immunol. 2022; 13:822576. https://doi.org/10.3389/fimmu.2022.822576 PMID: 35197986

77. Zhang Y, Planas D, Raymond Marchand L, Massanella M, Chen H, Wacleche VS, et al. Improving HIV Outgrowth by Optimizing Cell-Culture Conditions and Supplementing With all-trans Retinoic Acid. Front Microbiol. 2020; 11:902. https://doi.org/10.3389/fmicb.2020.00902 PMID: 32499767

78. Cicala C, Arthos J, Fauci AS. HIV-1 envelope, integrins and co-receptor use in mucosal transmission of HIV. J Transl Med. 2011; 9 Suppl 1:S2. https://doi.org/10.1186/1479-5876-9-S1-S2 PMID: 21284901

79. Santangelo PJ, Rogers KA, Zurla C, Blanchard EL, Gumber S, Strait K, et al. Whole-body immunoPET reveals active SIV dynamics in viremic and antiretroviral therapy-treated macaques. Nat Methods. 2015; 12(5):427–32. https://doi.org/10.1038/nmeth.3320 PMID: 25751144

80. Frank I, Cigoli M, Arif MS, Fahlberg MD, Maldonado S, Calenda G, et al. Blocking alpha4beta7 integrin delays viral rebound in SHIVSF162P3-infected macaques treated with anti-HIV broadly neutralizing antibodies. Sci Transl Med. 2021; 13(607).

81. Cory TJ, Schacker TW, Stevenson M, Fletcher CV. Overcoming pharmacologic sanctuaries. Curr Opin HIV AIDS. 2013; 8(3):190–5. https://doi.org/10.1097/COH.0b013e32835fc68a PMID: 23454865

82. Dyavar SR, Gautam N, Podany AT, Winchester LC, Weinhold JA, Mykris TM, et al. Assessing the lymphoid tissue bioavailability of antiretrovirals in human primary lymphoid endothelial cells and in mice. J Antimicrob Chemother. 2019; 74(10):2974–8. https://doi.org/10.1093/jac/dkz273 PMID: 31335938

83. Fletcher CV, Staskus K, Wietgrefe SW, Rothenberger M, Reilly C, Chipman JG, et al. Persistent HIV-1 replication is associated with lower antiretroviral drug concentrations in lymphatic tissues. Proc Natl Acad Sci U S A. 2014; 111(6):2307–12. https://doi.org/10.1073/pnas.1318249111 PMID: 24469825

84. Dobin A, Davis CA, Schlesinger F, Drenkow J, Zaleski C, Jha S, et al. STAR: ultrafast universal RNA-seq aligner. Bioinformatics. 2013; 29(1):15–21. https://doi.org/10.1093/bioinformatics/bts635 PMID: 23104886

85. Love MI, Huber W, Anders S. Moderated estimation of fold change and dispersion for RNA-seq data with DESeq2. Genome Biol. 2014; 15(12):550. https://doi.org/10.1186/s13059-014-0550-8 PMID: 25516281

86. Liberzon A, Birger C, Thorvaldsdottir H, Ghandi M, Mesirov JP, Tamayo P. The Molecular Signatures Database (MSigDB) hallmark gene set collection. Cell Syst. 2015; 1(6):417–25. https://doi.org/10.1016/j.cels.2015.12.004 PMID: 26771021